



User Manual

TOUGH2-GRS
Version 3

TOUGH2-MP-GRS
Version 1



Gesellschaft für Anlagen-
und Reaktorsicherheit
(GRS) gGmbH

User Manual

TOUGH2-GRS
Version 3

TOUGH2-MP-GRS
Version 1

Martin Navarro

December 2020

Remark:

This study has been funded by the German Federal Ministry for the Environment, Nature Conservation, and Nuclear Safety (BMU) under the support code no 4718E03260.

The work was conducted by the Gesellschaft für Anlagen- und Reaktorsicherheit (GRS) gGmbH.

The author is responsible for the content of the report.

GRS - 620
ISBN 978-3-949088-06-3

Keywords:

Flow, Simulation, TOUGH2, TOUGH2-GRS, TOUGH2-MP, TOUGH2-MP-GRS, Transport, Two Phase Flow

Kurzfassung

Die Codes TOUGH2 und TOUGH2-MP, die vom Lawrence Berkeley National Laboratory, Kalifornien, USA, entwickelt wurden, simulieren mehrphasige Strömungsvorgänge in porösen Medien. Die GRS verwendet TOUGH2-Codes seit 1991 im Rahmen von Prozess- und Langzeitsicherheitsanalysen für tiefe geologische Endlager und hat den Code im Laufe der Jahre um weitere, endlagerrelevante Prozesse erweitert. Im Vorhaben 4718E03260 des BMU wurden diese Entwicklungen fortgeführt. Der vorliegende Bericht aktualisiert das User Manual GRS-505 um die neuen Funktionalitäten der Codeversionen TOUGH2-GRS v. 3 und TOUGH2-MP-GRS v. 1.

Abstract

The codes TOUGH2 and TOUGH2-MP, which have been developed by the Lawrence Berkeley National Laboratory, California, USA, simulate multi-phase flow in porous media. GRS uses TOUGH2 codes since 1991 to conduct process analyses and safety assessments for deep geological repositories and it has added new processes to the code that are relevant to repository systems. Within BMU project 4718E03260, new developments have been made. The present report updates the previous user manual GRS-505 with the new functionalities of the code versions TOUGH2-GRS v. 3 and TOUGH2-MP-GRS v. 1.

Table of Contents

1	Introduction.....	1
2	General code features	3
2.1	Code basis.....	3
2.2	Major code versions.....	3
2.3	Differences between TOUGH2 and TOUGH2-MP	5
2.4	Deviations from TOUGH2 and TOUGH2-MP defaults.....	6
2.4.1	Unlimited number of materials (only TOUGH2-GRS).....	6
2.4.2	Unlimited number of time steps.....	6
2.4.3	Automatic Leverett scaling disabled.....	7
2.4.4	Extended printouts.....	7
2.4.5	Conservation of floating point precision (only TOUGH2-GRS)	7
2.4.6	Enforced solution of linear equations	8
2.5	Modules and physical processes	8
2.6	Handling porosity changes.....	11
2.7	Handling permeability changes	13
2.8	Restarting	13
3	New flow and transport features	17
3.1	Check valve boundary (IRP=9 in combination with an upstream weighting of mobilities).....	17
3.2	Simulated vertical pressure gradient (ICP=9 with IRP=1).....	17
4	CNTRL: Simulation controls	21
4.1	Termination controls	21
4.1.1	Do not exit on equilibrium (obsolete).....	21
4.1.2	Minimum time step width	21

4.2	Time step controls	22
4.2.1	Incrementing step widths	22
4.2.2	Avoiding convergence failures	22
4.2.3	Avoiding small time steps before printout times	22
4.2.4	Avoiding large changes in gas generation	23
4.3	Output controls	23
4.3.1	Precision of time series printouts	23
4.3.2	Reducing the amount of time series printouts	23
4.4	Input data	24
5	COMP: Convergence and compaction	25
5.1	Physical models.....	25
5.1.1	Change of cavity volume and porosity	25
5.1.2	Compaction rates.....	26
5.2	Note on the compaction of saturated media.....	28
5.3	Input data	28
6	CORFL	31
6.1	Implementation	31
6.2	Source and sink calculation	32
6.3	Degree of corrosion	33
6.4	Permeability change	34
6.5	Input data	35
7	CORRO: Gas production due to iron corrosion	37
7.1	Water consumption.....	37
7.2	Gas component	38
7.3	Gas generation rates	41
7.4	Input data	44

8	DEGRA: Time-dependent permeability changes	47
8.1	Model and implementation	47
8.2	Input data	47
9	DOFT	49
10	FISS: Gas pathway dilation	51
10.1	Pressure thresholds and softening models	51
10.2	Fissure porosity models	52
10.3	Permeability models	53
10.4	Input data	55
11	GCOMP: Primary non-condensable gas component	57
11.1	Absolute molecular weight	57
11.2	Specific enthalpy	57
11.3	Inverse Henry constant	58
11.4	Gas phase viscosity	58
11.5	Input data	60
12	PRLIM: Gas pressure limitation	61
12.1	Model and implementation	61
12.2	Input data	62
13	PTIME: High-precision printout times	63
14	RANGE: Limiting primary variables	65
14.1	Limiting brine mass fraction	65
14.2	Constant brine mass fraction	66

14.3	Clipping gas saturation and reducing vapour pressure	66
14.4	Input data	68
15	RELA: permeability and capillary pressure functions	69
15.1	Porosity-permeability relationships	69
15.2	Change of capillary pressures.....	69
15.3	Temperature-dependent capillary pressures.....	70
15.4	Input data	70
16	RN	73
16.1	Links to standard TOUGH2.....	73
16.2	Time stepping and performance	73
16.3	Simulation controls	75
16.4	Decay and adsorption of Nuclides	75
16.5	Anion exclusion	76
16.6	Extended mobilization models	79
16.6.1	New commands.....	79
16.6.2	Canister failure models	80
16.6.3	Bond models.....	83
16.6.4	Implementation	83
16.7	Input data	84
17	Output.....	87
17.1	Global printouts for elements (ELE_MAIN)	87
17.2	Global printouts for connections (CON_MAIN).....	90
17.3	Time series for elements (FOFT).....	92
17.4	Time series for connections (COFT)	94
17.5	Time series for sinks and sources (GOFT).....	95

17.6	Time series for domains (DOFT).....	96
	References	97
	List of Figures.....	103
	List of Tables	105
	Acknowledgements.....	107

1 Introduction

TOUGH2 is a code for the simulation of multi-phase flow in porous media that was developed at the Lawrence Berkeley National Laboratory, California, USA /PRU 99/. TOUGH2-MP /ZHA 08/ is a multi-processor version of TOUGH2. GRS uses both codes to simulate multi-phase flow and radionuclide transport in repository systems for radioactive waste.

Since 1992, GRS is extending TOUGH2 by physical processes that are relevant to repository systems. Early code modifications focused on repository concepts for rock salt and included porosity and permeability changes due to salt creep /JAV 95/, which is a driving process for barrier sealing in such concepts. Non-linear and brine-dependent sorption was implemented to simulate the transport of radionuclides in the far-field of a repository /JAV 01/, /JAV 02/, /FIS 01/. The focus then shifted to argillaceous host rocks. From 2006 to 2008, a porosity model for immobile water was introduced /NAV 08/ as well as the process of dilating micro fissures, known under the name pathway dilation /NAV 09/. The pathway dilation model was applied in the FORGE project to explain gas injection experiments conducted in the Mont Terri underground research laboratory /NAV 13a/. In the project, new mechanisms of pathway dilation including kinetic dilation processes were added.

Until 2009, most additions to the TOUGH2 code were realized independently. Integration and improvement of previous modifications was attempted between 2009 and 2012 in BMU project 3609R03210, resulting in the code TOUGH2-GRS version 0 /NAV 13b/. This code was extensively used in the VSG project, a preliminary safety analysis for the Gorleben site (BMU project UM10A03200, /LAR 13/, /KOC 12/).

The shift to version 1 /NAV 16a/, was undertaken in project ZIESEL (UM13A03400, /KOC 16/). The code version was subject to extensive quality assurance, particularly by means of the automatic code testing programme SITA developed by GRS /SEH 16/, /NAV 18a/, /HOT 17/.

In BMU project 4715E03230, anion exclusion and temperature-dependent capillary pressures were introduced to the code. All code extensions were ported to the multi-processor code TOUGH2-MP forming the new code TOUGH2-MP-GRS. Both codes, TOUGH2-GRS and TOUGH2-MP-GRS, are described in this report, which updates the previous user manuals /NAV 16a/ and /NAV 18b/. Most features of TOUGH2-MP-GRS resemble the features of TOUGH2-GRS, so that most parts of this report apply to both codes. Exceptions from this rule are mentioned.

2 General code features

2.1 Code basis

The code TOUGH2-GRS is based on the code TOUGH2, version 2.0, and on the solver package T2SOLV (files t2cg22.f and t2solv.f) of TOUGH2 version 2.1. Bugfixes for TOUGH2 v. 2.0 were published on the LBNL website /LBNL 16/ and included in TOUGH2-GRS.

We have modified the solver package T2SOLV of TOUGH2 to speed up the iterative solvers DSLUBC, DSLUCS, DLUSTB, and DSLUGM. This modification improves the transformation from coordinate format (COO) to compressed sparse column format (CSC) by changing the routines DS2Y and QS2I1D. The modified solver package was presented at the TOUGH-Symposium 2015 /NAV 15/ and has shown to yield a significant speed improvement of about 25 – 30 % /JUN 17/.

The code TOUGH2-MP-GRS, version 0, was built by porting the GRS code extensions of TOUGH2-GRS to TOUGH2-MP, version 2.0.

2.2 Major code versions

Full version names of TOUGH2-GRS and TOUGH2-MP-GRS take the form

`<major version>.<minor version>.<patch version>.`

The major code version is assigned to specific code development projects. The minor version indicates code compatibility. Source codes sharing the same minor version must be compatible with regard to functionality, input and output parameters. Patch versions introduce bug-fixes or minor code changes. This report only refers to major code versions.

TOUGH2-GRS v. 0

The main achievement of this code version was to integrate previous lines of code development into a single code. The code was developed in BMU project UM10A03200 (VSG) /NAV 13b/.

TOUGH2-GRS v. 1

Version 01 of TOUGH2-GRS was subject to a major restructuring and benefited from a highly modular structure. New physical processes (called process modules) were added and the implementation of existing modules was substantially changed. All physical process modules (except for modules PRLIM and RN) were included in the implicit Newton-Raphson solution scheme to yield higher accuracy. Version 1 introduced non-comprehensive plausibility checks for input data as well as a reporting system for messages, warnings and errors. The code developments were conducted in BMU project UM13A03400 (ZIESEL) /NAV 16a/.

TOUGH2-GRS v. 2

The version, which was developed in BMU project 4715E03230, introduced the following features:

- Temperature-dependent capillary pressures
- Anion exclusion for module RN
- Controls for the Burlirsch-Stoer solver of the RN module
- Irreversible softening for module FISS
- Porosity-dependent permeabilities and capillary pressures can be set by the new module RELA

The coupling of the TOUGH2 with the geomechanical code FLAC3D, called TFC, has been a stand-alone code before. It is now part of TOUGH2-GRS. Since TFC requires a serial version of TOUGH2 it is not part of the parallel TOUGH2-MP-GRS code.

TOUGH2-MP-GRS v. 0

In BMU project 4715E03230, most of the code extensions of TOUGH2-GRS were ported to the code TOUGH2-MP /ZHA 08/. The general code structure of the ported code parts was left unchanged but additional routines were implemented for the exchange of data between processes. Read and write operations are only carried out by process 0 which requires inter-process communication for the distribution and collection of data. The RN module demands additional process communication owing to the flow calculations it performs.

TOUGH2-GRS v. 3 and TOUGH2-MP-GRS v. 1

A restart functionality was added to both codes and new plausibility checks for input data were developed. Both source codes were consolidated. This included a partial restructuring of the code, elimination of unused code parts and an update of source code comments. Output routines were harmonised to reduce the susceptibility of the code to coding errors. Array and Functions of TOUGH2-MP-GRS that convert local to global indices or vice versa were brought together in a new module called INDICES to provide a better overview on the indexing system. Several modules of TOUGH2-GRS were adjusted to those of TOUGH2-MP-GRS in order to unify the structure of both codes.

2.3 Differences between TOUGH2 and TOUGH2-MP

The following features of TOUGH2-MP /ZHA 08/ differ from the serial TOUGH2 code.

- Zero volume elements are no longer used for the definition of inactive elements. Large-volume elements are mandatory.
- ICP = 8 selects the ECM capillary pressure function and ICP = 9 a generalized ECM function (see /ZHA 08/ for details). In contrast, ICP = 8 of the TOUGH2 code means “no capillary pressure”.
- ICP = 9, 10 selects the ECM function (see /ZHA 08/ for details).
- For T2R3D, an additional rock card is required with radionuclide specific transport properties.
- MOP(10): A new interpolation formula for heat conductivity can be selected by MOP(10)=2.
- MOP(14): This switch specifies if 5- or 8-character elements are used. Zero stands for 5-character elements. The choice affects the length of strings for elements and connections used in the input blocks ELEME, CONNE, GENER, INCON, FOFT, COFT, and GOFT.
- MOP(15) = 1 (heat exchange in TOUGH2) has no function in TOUGH2-MP.
- MOP(17) allows to generate a file holding T2R3D transport simulations for EOS9.

- MOP(20) controls the format of CONNE and GENER indexes (0 uses format 16I5 and 1 uses format 10I8).
- If REDLT < 0 is chosen –REDLT is used as increasing rate for time-step size.
- NELIST and EPLIST(I) are used to print time series of primary variables for selected elements.
- Card TIMBC introduces a table for time-dependent pressure boundary conditions.
- Card RTSOL introduces additional parameters for time stepping, iteration and solvers.

These features have remained unchanged in TOUGH2-MP-GRS except for the roll-back to the original ICP = 8 (“no capillary pressure”) feature.

Note that TOUGH2-MP requires at least 4 elements and 3 connections.

2.4 Deviations from TOUGH2 and TOUGH2-MP defaults

2.4.1 Unlimited number of materials (only TOUGH2-GRS)

TOUGH2-GRS still uses static array sizes. The maximum number of materials can be adjusted by parameter MR, which is located in file `module_sizes.f90`. Note that MR must be *larger* than the number of materials in use because of the specific coding of the TOUGH2 input routine, which has remained unchanged.

2.4.2 Unlimited number of time steps

Parameter MCYC defines the maximum number of time steps. The default value MCYC=0 forces TOUGH2 v. 2.0 to quit the simulation before the first time step. On the contrary, TOUGH2-GRS uses MCYC=0 to indicate the absence of a time step limit. Input files of TOUGH2-GRS therefore cannot be used with TOUGH2 v. 2.0 if MCYC = 0.

2.4.3 Automatic Leverett scaling disabled

In contrast to TOUGH2 v. 2.0 there is no automatic Leverett scaling of capillary pressures if permeability modifiers (P_M) are used.

2.4.4 Extended printouts

TOUGH2-GRS and TOUGH2-MP-GRS generate additional printout at time zero and after the last time step. The default value of parameter $MCYPR$ ($MCYPR=0$) defining the maximum time step difference between two printouts has been changed from 1 to 10^7 .

Element and connection specific printouts are directed to the output files `ELE_MAIN` and `CON_MAIN` using the data format of the time series files `FOFT`, `COFT`, and `GOFT`.

The printout of total component masses in active elements (the printout that starts with "MASS IN PLACE") is now a printout for elements with volume smaller than $1E+50$ m³.

2.4.5 Conservation of floating point precision (only TOUGH2-GRS)

Input data are read by TOUGH2 v. 2.0 either from the STDIN channel or from separate files like the MESH file. If input data is passed via the STDIN channel, the data will first be written to a separate file and reread afterwards. This indirect reading of input data may cause a loss of floating point precision.

Read and write operations of TOUGH2 v. 2.0 are performed using the format string "E10.4". This causes a loss of precision if the user makes efficient use of the field length. Let us consider the read and write operations for the element volume, which is stored in the ELEM data block. Reading a numerical value of $1.23456E+4$ from the STDIN channel by means of the format string "E10.4" is not a problem, but writing this value to the MESH with the same format string yields $0.1235E+05$ if the gfortran 4.9.3 compiler is used. Apparently, the introduction of leading zeros to the significand and exponent has resulted in a loss of two digits. TOUGH2-GRS solves this problem by reading and writing strings ("A10") instead of floating point values.

2.4.6 Enforced solution of linear equations

If convergence is achieved in the cycle of the Newton-Raphson iteration, primary variables remain unchanged because the linear equations are not solved. As a consequence sources and sinks (which are introduced by adding a term to the right side of the linear equation system) remain inactive. Usually, this is not a problem because the convergence criteria are met. However, the absence of sinks and sources can cause problems in connection with the CORFL, COMP and CORRO modules of TOUGH2-GRS, which are introducing sinks and sources. The processes of these modules are stalled if convergence is achieved in the first cycle and this might sum up to significant errors with time. TOUGH2-GRS and TOUGH2-MP-GRS therefore enforce at least two iterations ($ITER > 1$). The related MOP(21) switch of TOUGH2-MP-GRS was deactivated.

2.5 Modules and physical processes

TOUGH2-GRS and TOUGH2-MP extensions are organized in Fortran modules as shown in Tab. 2.1. Some modules introduce new input data block named after the module's name. All modules were developed for the use with the EOS7 and EOS7R although the combination TOUGH2-MP-GRS/EOS7R has not been extensively tested.

Fortran modules cannot use each other in a circular manner. To clarify module dependencies, modules are grouped in ten levels according to Tab. 2.1. Modules are only allowed to use modules of a lower level. The compilation of modules must proceed from the lowest to the highest level.

Modules COMP, CORFL, CORRO, DEGRA, FISS, GCOMP, PRLIM, RELA and RN introduce new physical processes or properties. We will refer to these modules as "process modules".

Some process modules do not only change porosity but also require information on the current porosity estimation of other process modules. For this reason, variables holding porosity changes were ported from the process modules to module PORO. As a lower-level module, PORO can be accessed by every process module to obtain information on porosity change estimates of other process modules. The PORO module includes shared routines for porosity handling as well as a routine for the reduction of connection interfaces due to compaction (see also chapter 2.6).

Permeability changes are managed differently from porosity changes because process models do not need to know about the permeability estimates of other process modules. For this reason, the permeability change module PERM is a high-level module. It collects permeability changes induced by process modules and passes them to the TOUGH2 core.

Tab. 2.1 Fortran modules of TOUGH2-GRS and TOUGH2-MP-GRS

Modules in bold face introduce new data blocks. Data block keywords correspond to the module names.

Level	Fortran modules of the code extension		Purpose
	TOUGH2-GRS	TOUGH2-MP-GRS	
10	PROGFLOW	PROGFLOW	High-level routines used as an interface for the TOUGH2 and TOUGH2-MP cores
9	TEST	TEST	Plausibility tests for input data
	OUTPUT	OUTPUT	Extended output
	ANALYSE	-	Run-time monitoring for the physical interpretation of convergence failures
	NEWBLOCKS	NEWBLOCKS	General routines for new input data blocks
8	PERM	PERM	General permeability routines and externalized permeability variables
7	CNTRL	CNTRL	General controls including time step control
	COMP	COMP	Compaction of crushed salt backfill in rock salt cavities including changes of permeability and capillary pressure
	CORFL	CORFL	Seal corrosion by corroding fluids
	CORRO	CORRO	Gas production and water consumption due to metal corrosion
	DEGRA	DEGRA	Time-dependent change of seal permeability
	DOFT	DOFT	Time series for domains (rocks)
	FISS	FISS	Transport of gas in microscopic pathways including porosity and permeability changes, pressure thresholds, softening mechanisms and kinetic effects
	GCOMP	GCOMP	Properties of the main gas component of EOS7(R)
	PRLIM	PRLIM	Pressure limitation caused by the escape of gas from the model domain
	PTIME	PTIME	TIME vector with higher precision
	RN	RN	Decay, advection, diffusion, linear sorption and anion exclusion for radionuclide chains
RANGE	RANGE	Limits primary variables	
6	RELA	RELA	Functional dependencies for permeability and capillary pressure
5	PORO	PORO	General routines for porosity change and externalized porosity variables
4	ALARM	ALARM	Reporting system for messages, warnings, and errors
	-	TIMER	Time measurement
3	MISC	MISC	General constants and routines
2	TOUGH	MODULES	Gives access to global TOUGH2 variables
1	SIZES	<i>(not needed)</i>	Static TOUGH2 array sizes

2.6 Handling porosity changes

Porosity changes that are caused by matrix compression and thermal expansion are basic parts of TOUGH2-based codes. TOUGH2-GRS and TOUGH2-MP-GRS also consider porosity changes induced by backfill compaction (module COMP, see chapter 4) and opening of micro fissures by the gas phase (module FISS, see chapter 9).

Porosities are changed in the standard way: First, porosity is changed by setting a porosity $\phi_{\text{PHI}(N)}$ to its new value. This is done without touching other variables like for instance gas saturation. Changing porosity leads to an unphysical change of component masses, which is corrected by introducing sinks or sources for the respective components. This is an efficient way to model porosity changes that do not happen instantaneous but are coupled to flow processes.

Every Newton-Raphson iteration calculates a new porosity estimation ϕ_{tough} . Several processes can contribute to the change of porosity in the time step $\Delta\phi_{\text{tough}}$. These are backfill compaction ($\Delta\phi_{\text{comp}}$), opening of micro-fissures ($\Delta\phi_{\text{fiss}}$), rock compaction and thermal expansion ($\Delta\phi_{\text{ce}}$)

$$\Delta\phi_{\text{tough}} = \Delta\phi_{\text{ce}} + \Delta\phi_{\text{comp}} + \Delta\phi_{\text{fiss}} \quad (2.1)$$

Porosity changes due to rock compaction and thermal expansion usually are small, so that the changes of element volume can be neglected. However, porosity changes caused by backfill compaction ($\Delta\phi_{\text{comp}}$) can considerably alter the volume of an element. Since the TOUGH2 variable for the element volume V_{evol} is a constant (called V_{tough} in the following) a new variable $V_{\text{phys}}(t)$ is introduced, which is the physical volume of the compacting material. $V_{\text{phys}}(t)$ is accompanied by a new porosity variable for the porosity of the compacting domain ϕ_{phys} .

The volume and porosity variables of TOUGH2, V_{tough} and $\phi_{\text{tough}}(t)$, are related to the new volume and porosity variables TOUGH2-GRS and TOUGH2-MP-GRS by the assumption of pore space conservation:

$$V_{\text{phys}}(t) \cdot \phi_{\text{phys}}(t) = V_{\text{tough}} \cdot \phi_{\text{tough}}(t) \quad (2.2)$$

$V_{\text{cavity}}(t)$ and $\phi_{\text{tough}}(t)$ are updated every Newton-Raphson iteration assuming that the change of element volume equals the change of pore volume:

$$V_{\text{cavity}}(t) = V_{\text{cavity}}(t_{\text{old}}) + V_{\text{tough}} \cdot \Delta\phi_{\text{comp}} \quad (2.3)$$

$$\phi_{\text{tough}}(t) = \phi_{\text{tough}}(t_{\text{old}}) + \Delta\phi_{\text{ce}} + \Delta\phi_{\text{comp}} + \Delta\phi_{\text{fiss}}, \quad (2.4)$$

where t_{old} is the time after the last successful time step.

By definition, fissure porosity ϕ_{fiss} is only accessible to gas (see chapter 9) so that capillary pressures should vanish if the liquid-accessible porosity $\phi_{\text{phys}} - \phi_{\text{fiss}}$ is saturated. Capillary pressure functions of TOUGH2-GRS and TOUGH2-MP-GRS therefore depend on the liquid saturation not of the total but of the liquid-accessible porosity \hat{S}_{liq} . The liquid-accessible porosity is

$$\hat{S}_{\text{liq}} = S_{\text{liq}} \cdot \left(1 - \frac{\phi_{\text{fiss}}}{\phi_{\text{phys}}}\right)^{-1}, \quad (2.5)$$

which is derived from the relation

$$S_{\text{liq}} \cdot \phi_{\text{phys}} \cdot V_{\text{phys}} = \hat{S}_{\text{liq}} \cdot (\phi_{\text{phys}} - \phi_{\text{fiss}}) \cdot V_{\text{phys}} \quad (2.6)$$

Large changes of porosity and element volume should be considered in the flow section of element connections. Changing interface areas would require the introduction of a separate weighting scheme for interface areas. We avoid this by multiplying permeabilities, diffusivities, and thermal conductivities of elements by a correction factor

$$\frac{A_t}{A_0} \quad (2.7)$$

with A_0 being the interface area of the connection and A_t the true interface area at time t . To calculate A_t/A_0 we assume that rock convergence is the chief contributor to volume change and that drifts are the most important structures to be considered. Convergence of a drift takes place in two dimensions so that we can set

$$\frac{A_t}{A_0} = \frac{V_t}{V_0}, \quad (2.8)$$

where V_0 is the initial element volume and V_t is the true volume at time t . Note that this relation is based on the above-mentioned assumptions.

2.7 Handling permeability changes

Modules DEGRA and CORFL introduce time-dependent changes of intrinsic permeability by means of the permeability factors f_{DEGRA} and f_{CORFL} , respectively. If defined, the isotropic porosity-permeability relation $k_{\text{RELA}}(\phi)$ of module RELA substitutes the anisotropic permeability \vec{k}_{ROCKS} of data block ROCKS:

$$\vec{k} = \begin{cases} |f_{\text{PM}}| f_{\text{DEGRA}} f_{\text{CORFL}} k_{\text{RELA}}(\phi) \mathbf{I} & \text{if } k_{\text{RELA}}(\phi) \text{ is defined and } f_{\text{PM}} \geq 0 \\ |f_{\text{PM}}| f_{\text{DEGRA}} f_{\text{CORFL}} \vec{k}_{\text{ROCKS}} & \text{otherwise} \end{cases} \quad (2.9)$$

Permeability modifiers f_{DEGRA} and f_{CORFL} are set to 1 if the respective module is inactive. f_{PM} is the TOUGH2 permeability modifier PM of data block `ELEME`. In equation (2.9), we use the absolute value of f_{PM} because the RELA module uses negative values of f_{PM} as a switch to turn off the porosity-permeability relationship $k_{\text{COMP}}(\phi)$ for single elements.

Module FISS introduces a new permeability term to the flow equation of the gas phase without changing intrinsic permeability \vec{k} . This is explained in chapter 10, see equation (10.14) on p. 53.

2.8 Restarting

Restart files with information on state variables are created at every printout time. Time, timestep, porosity, and the state of primary variables are stored, as usual, in the restart file `SAVE`. Some process modules of TOUGH2-GRS and TOUGH2-MP-GRS create additional restart files, which follow the naming convention `SAVE_<module name>`. These have to be renamed (the string “SAVE” has to be replaced by “INCON”) and copied to the simulation directory for a restart. Tab. 2.2 shows the content of all restart files.

Restart files can be selected and modified to control which data is loaded at the restart. If the restart file `SAVE` remains unchanged the simulation resumes the time step of the last printout. Replacing line ‘+++’ with a blank line resets the time to 0. Module specific restart files `SAVE_<module name>` can be edited too. Here, every line may be deleted except for lines that hold parameter names or start with a zero. Module specific restart files usually store state parameters in the following way.

```

<name of parameter>
<global element index> <value>
<global element index> <value>
...
0 0.0
<name of parameter>
<global element index> <value>
<global element index> <value>
...
0 0.0

```

In restart file SAVE_CORRO, some values are assigned to element-source pairs leading to a somewhat different data structure:

```

<name of parameter>
<global element index> <source> <value>
<global element index> <source> <value>
...
0 0 0.0

```

Modules like RN store two-dimensional state arrays. These are split up and stored as a sequence of one-dimensional arrays in the following way:

```

<name of parameter>-1
...
<name of parameter>-2
...

```

Tab. 2.2 Restart files and their content

Restart File	Content
SAVE	porosity, primary variables, time step, time (sec), iteration counters
SAVE_COMP	physical element volume (m ³), porosity (overwrites porosities of SAVE)
SAVE_CORFL	mass density of generated brine (kg/m ³)
SAVE_CORRO	degree of corrosion, canister water mass (kg), produced gas (mole)
SAVE_FISS	fissure porosity, pressure threshold (Pa)
SAVE_PRLIM	gas mass that has escaped from the system (kg), gas volume that has escaped from the system (m ³)
SAVE_RN	amount of radionuclides (mole)

Restart file SAVE_COMP includes porosity information which is also stored in SAVE. The reason is that it has to be ensured that porosity information remains consistent if the restart file SAVE is not in use. If present, input blocks set or overwrite porosity data in the following order: ROCKS → INCON → INCON_COMP.

A restart of module DEGRA requires that the simulation continues at the last time. This requires the SAVE file. Modules GCOMP, RELA, RANGE, and CNTRL do not require any restart files.

TOUGH2-GRS and TOUGH2-MP-GRS do not check for the plausibility of changes in the restart files. To avoid inconsistent simulations, the following should remain unchanged.

- The number of elements
- Element indices (as defined by ELEME)
- The number and sequence of sources if module CORRO is used
- The number and sequence of radionuclides if module RN is used

The following should only be changed if the user knows what he or she is doing.

- The corrosion models of module CORFL
- The fissuring models of module FISS

It is always possible to activate or deactivate process modules when restarting.

3 New flow and transport features

3.1 Check valve boundary (IRP=9 in combination with an upstream weighting of mobilities)

Flow boundaries can be designed as one-way outlets (a check valve behaviour) by defining inactive elements with zero permeability. However, this approach works only if intrinsic permeabilities are upstream-weighted. With harmonic weighting a vanishing permeability no advective flow would be possible.

In connection with a harmonic weighting of permeabilities, one-way outlets can now be introduced by choosing upstream weighted mobilities ($MOP(11) = 2$) and applying the new permeability function $IRP = 9$ to inactive elements. $IRP = 9$ sets the relative permeability to zero for all phases, so that fluids can only flow into the boundary but not leave it.

3.2 Simulated vertical pressure gradient (ICP=9 with IRP=1)

If the host rock of a repository is impermeable rock salt it usually does not have to be included in the modelling grid. Consequently, the modelling grids for such repositories usually are networks of mining cavities, namely drifts, chambers and shafts.

Acceptable simulation times for repositories in rock salt can often be achieved by a coarse spatial discretization. One possibility to do so is to model horizontal drifts as one-dimensional structures without vertical discretization. This approach saves computation time but must be used with caution because it can introduce the wrong physics.

Without vertical discretization no gravitational flow takes place. Consequently, the gas phase will not ascend to the top of the drift but remain homogeneously distributed in vertical direction. The hydraulic behaviour of such a system can differ significantly from systems with gravitational flow that allow for a vertical separation of phases. Let us consider the case of a gas bubble that has been trapped in front of a gastight seal. If vertical phase separation was possible, the gas bubble would ascend and accumulate at the top of the drift, allowing the liquid phase to pass by. But without vertical phase separation, the gas phase would remain homogeneously distributed and block the flow of liquid through the seal.

It is still possible to simulate a vertical separation of phases within drifts even if there is no vertical discretisation. This can be achieved by substituting the missing gravitational forces by capillary forces. TOUGH2-GRS and TOUGH2-MP-GRS introduce a new capillary pressure function ($I_{CP} = 9$), which adds a correction term to the van Genuchten capillary pressure function. The purpose of the correction term is to compensate for the lack of gravitational forces that is caused by the missing vertical discretisation.

To derive the correction term we examine the two flow systems shown in Fig. 3.1. Both systems are closed systems with constant initial gas pressure and no capillary forces. System A is composed of two grid elements with gas saturation S_{g1} and S_{g2} . System B is derived from system A by subdividing the elements in vertical direction. The mean gas saturation of domain 1 and 2 in system B shall be equal to the gas saturation of element 1 and 2 in system A, respectively.

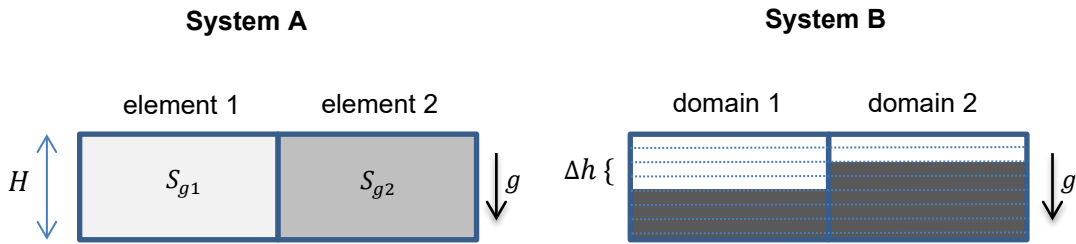


Fig. 3.1 Models for drift sections with (A) and without (B) vertical discretisation
 g : gravity, H : drift height, Δh : height difference of water columns, S_g : gas saturation.

System B establishes a liquid flow from domain 2 to domain 1 because of the pressure difference

$$\Delta p_{2 \rightarrow 1} = -\rho g \Delta h (S_{g2} - S_{g1}) \quad (3.1)$$

induced by the height difference of both water columns (note that S_{g1} and S_{g2} refer to a gas and not to a liquid saturation). Here, ρ is the liquid density, g the gravitational acceleration and Δh the height difference between the water columns.

In contrast to system B, system A will not establish a liquid flow because of the equal pressures at the element centres. To initiate the same flux as in system B, a correction pressure

$$p_{\text{grav}}(S_g) := -\rho g H S_g \quad (3.2)$$

is introduced, which leads to the desired pressure difference

$$\Delta p_{\text{grav},2 \rightarrow 1} = -\rho g \Delta h (S_{g2} - S_{g1}). \quad (3.3)$$

We add the correction pressure to the capillary pressure function $p_{\text{cap}}(S_g)$ to construct a corrective capillary pressure

$$\hat{p}_{\text{cap}}(S_g) = p_{\text{cap}}(S_g) + p_{\text{grav}}(S_g), \quad (3.4)$$

which compensates for the missing gravitational effects in drifts without vertical discretisation. Note that TOUGH2 uses negative capillary pressures. If $p_{\text{cap}}(S_g)$ is the van Genuchten function /GEN 80/, \hat{p}_{cap} can be selected by setting $\text{ICP} = 9$. The input parameters $\text{CP}(1)$ to $\text{CP}(5)$ are the same as for the van Genuchten function ($\text{ICP} = 7$). The additional parameter $\text{CP}(6)$ holds the term $\rho g H$.

To account for the linear dependency between the flow section and saturation a linear relationship for the relative permeabilities should be used ($\text{IRP} = 1$), see /NAV 16b/.

4 CNTRL: Simulation controls

The CNTRL module holds various simulation controls related to termination criteria, automatic time stepping, and printing. The structure of data block CNTRL is shown in Tab. 4.1.

4.1 Termination controls

4.1.1 Do not exit on equilibrium (obsolete)

TOUGH2 v. 2.0 uses two criteria for the detection of static or dynamic equilibria. The code terminates if either ten iterations with `ITER=1` have occurred or if there is a convergence failure after two subsequent iterations with `ITER=1`. In version 00 of TOUGH2-GRS, the CNTRL module allowed to disable these criteria by using the two parameters `cntrl_ignore10TimesIterEq1` and `cntrl_ignoreConvFailureAfter2TimesIterEq1`. This feature is obsolete since TOUGH2-GRS v. 01 due to the enforcement of at least two iterations (see chapter 2.4.6).

4.1.2 Minimum time step width

Some process modules can induce high fluxes. The CORFL module, for instance, can trigger rapid flow processes after seal failure. Fast processes usually cause a drastic reduction of time step widths to a degree where simulations become inefficient and should be terminated. To avoid stagnant simulations with unreasonably small step widths, the parameters `minStepSize` and `stopAfter` can be used terminate the execution as soon as the time step width falls below `minStepSize` for `stopAfter` successive time steps.

4.2 Time step controls

4.2.1 Incrementing step widths

TOUGH2 increases time step widths if the number of Newton-Raphson iterations `ITER` is smaller than or equal to `MOP(16)`. The standard increasing factor is 2 but can now be adjusted by means of parameter `dtfacQuickIter`.

The fact that TOUGH2 stops to increase step widths if $ITER > MOP(16)$ means that the bandwidth of time steps meeting the criterion $NOITE \geq ITER > MOP(16)$ is not sufficiently explored. The automatic time stepping control of TOUGH2 works fine if this bandwidth remains small. However, there are cases where the bandwidth is large and should be explored by the automatic time stepping control. This can now be achieved by setting parameter `dtfacSlowIter` with $1 \leq dtfacSlowIter < dtfacQuickIter$. Parameter `dtfacSlowIter` is the increasing factor for time step widths in case of $NOITE \geq ITER > MOP(16)$.

4.2.2 Avoiding convergence failures

If the bandwidth of time steps meeting the criterion $NOITE \geq ITER > MOP(16)$ is too small or even zero, the performance of the simulation will suffer from too many convergence failures. In order to avoid this, TOUGH2-GRS and TOUGH2-MP-GRS can be instructed to avoid the last time step width that has produced a convergence failure for at least `cntrl_avoiddt` time steps.

4.2.3 Avoiding small time steps before printout times

Printout times introduced by data blocks `TIMES` and `PTIMES` can lead to a drastic reduction of time step widths because overshooting time steps have to be clipped to reach the specified printout time.

Setting `cntrl_softlanding = 1` activates an automatic step width adjustment to attenuate this effect. If activated, it is checked whether the next printout time is nearer than a quadruple of the current time step size and if so, the step width is slightly reduced with the aim of dividing the time to the next printout into four almost equal parts.

4.2.4 Avoiding large changes in gas generation

If sinks and sources are introduced using interpolated tabular data ($MOP(12)=0$) large time steps can lead to an inaccurate mass injection or production. Setting parameter `cntrl_MaxRelGenRateChange` to a positive value reduces the time step width in a way that changes of generation rates remain smaller than parameter `cntrl_MaxRelGenRateChange` (rate change per rate).

4.3 Output controls

4.3.1 Precision of time series printouts

Data blocks FOFT, COFT and GOFT introduce time series printouts for specified elements, connections, and sources, respectively. TOUGH2-GRS and TOUGH2-MP-GRS introduce additional domain-specific printouts by means of data block DOFT (see chapter 16.6).

Time series printouts can be very large if there are a lot of time steps. The file size can be controlled by parameter `cntrl_decimalplaces`, which adjusts the number of decimal places. (Note that values of 0 and 1 will always be printed as "0." and "1.", respectively, no matter how many decimal places are prescribed.) A negative value of `cntrl_decimalplaces` converts the printout to binary format using the output files `FOFT.bin`, `COFT.bin`, `GOFT.bin`, and `DOFT.bin`. These files can be converted to ASCII format by means of the tool `translate.f90`.

4.3.2 Reducing the amount of time series printouts

An effective way of decreasing the size of time series printouts is to skip time steps. Parameter `cntrl_ioft` defines a minimum time step difference between successive printouts. Parameter `cntrl_MinRelDur` multiplied by the current time gives the minimum time between successive printouts.

4.4 Input data

Tab. 4.1 shows the structure of data block CNTRL.

Tab. 4.1 Input format of data block CNTRL

Line	Column	Content	Format	Unit	Description	Variables (Long names! Ignore line feeds.)
1	1-5	"CNTRL"	A5		Keyword	
w2	1-10	Do not stop after 10 iterations with ITER=1?	I10		0: no 1: yes	cntrl_ignore10 TimesIterEq1
2	11-20	Do not stop after convergence failure subsequent to two iterations with ITER=1?	I10		0: no 1: yes	cntrl_ignore ConvFailure After2Times IterEq1
3	1-10	Stop execution if time step width remains N times below T_{min} ?	G10.4	sec	T_{min} (inactive if equal 0)	minStepSize
3	11-20		I10		N	stopAfter
4	1-10	Factor for the increase of time step width if $ITER < MOP(16)$	G10.4		default: 2 recommended: 1.2	cntrl_dtfac QuickIter
4	11-20	Factor for the increase of time step width if $ITER \geq MOP(16)$	G10.4		default: 1 recommended: 1.1	cntrl_dtfac SlowIter
5	1-10	Number of time steps that avoid last time step width with convergence failure	I10		0: inactive	cntrl_avoiddt
6	1-10	Adapt time stepping in order to avoid small time step widths before printout times	I10		0: no 1: yes	cntrl_ softlanding
7	1-10	Maximum relative change of the generation rate if linear interpolated tables are used (rate change per rate)	G10.4		0: inactive	cntrl_MaxRel GenRateChange
8	1-10	Decimal places of real numbers	I10		0: switches to 12, <0: binary output	cntrl_decimal places
9	1-10	Stride for time series printouts (FOFT, COFT etc.)	I10		0: switches to 1 (=print every time step)	cntrl_ioft
10	1-10	Minimum time between two time series printouts divided by time	G10.4		0: inactive	cntrl_MinRelDur
11	1-10	Printout run-time information to STDOUT (not in use anymore)	I10		0: no 1: yes	cntrl_ monitoring

5 COMP: Convergence and compaction

Rock salt is subject to creep deformation. Mining cavities in rock salt therefore contract with time. This process is usually called "convergence" because the walls of a spherical cavity tend to converge against one point. The rate of convergence depends on the support of the backfill, if present, but also on the fluid pressure within the cavity. Convergence compresses the backfill and reduces its porosity as well as its permeability. Capillary pressures and relative permeabilities may change too.

The COMP module implements the combined process of convergence and backfill compaction. The mathematical model will only be described briefly in this report. Further details on the origin and purpose of the model can be found in /NAV 13c/ in German language.

5.1 Physical models

5.1.1 Change of cavity volume and porosity

According to /STE 85/ the volume change of a cavity with volume $V(t)$ due to convergence can be described by the differential equation

$$\dot{V}(t) = -K \cdot V(t) \quad (5.1)$$

Factor $K > 0$ is called the rate of convergence and depends on the local pressure, porosity, and temperature. Volume V is the volume of an entire cavity and is not to be confused with the volume of grid elements used for the discretisation of that cavity. However, if a homogeneous distribution of K in the backfill is assumed, equation (5.1) also describes the compaction of a subvolume i of the cavity (a grid element, for example):

$$\dot{V}_i = -K \cdot V_i \quad \text{with} \quad \sum_i V_i = V. \quad (5.2)$$

Factor K of equation (5.2) does not refer to the convergence of a cavity anymore but to the convergence of a grid element, which is part of a converging cavity. We therefore

call K of equation (5.2) a *rate of compaction*, not a rate of convergence. TOUGH2-GRS and TOUGH2-MP-GRS apply equation (5.2) using the physical volume variable described in chapter 2.6.

5.1.2 Compaction rates

Compaction rates are calculated using a slightly modified approach of /NOS 05/. In /NAV 13c/, this approach is called the "extended approach of Stelte". Here, the convergence rate is derived from a *reference convergence rate* K_{ref} by applying factors for the dependencies of the convergence rate on location, pressure, backfill porosity, time, and temperature. (Note that we set compaction rates equal to convergence rates.)

$$K = \begin{cases} K_{\text{ref}} \cdot f_{\text{loc}} \cdot f_p \cdot f_\phi \cdot f_t \cdot f_T & \text{for } \phi > \phi_{\text{lim}} \\ 0 & \text{for } \phi \leq \phi_{\text{lim}} \end{cases} \quad (5.3)$$

Variable ϕ_{lim} is a lower porosity limit, which is not part of the extended approach of Stelte. The factors of the term belonging to $\phi > \phi_{\text{lim}}$ are the following.

- **Reference convergence rate.** It has been assumed by Stelte that the convergence rate of an open cavity converges against a constant value, the *stationary convergence rate* /NAV 13c/. The reference convergence rate K_{ref} is the stationary convergence rate of an open cavity at reference conditions $p_{\text{ref}} = 1$ bar (the reference gas pressure in the cavity) and T_{ref} (the temperature of the surrounding rock). The reference convergence rate can be estimated from in-situ measurements or geo-mechanical simulations.
- **Local dependency.** f_{loc} captures spatial dependencies of the stationary convergence rate. The stationary convergence rate usually varies with depth, temperature, and geometry of the cavity.
- **Pressure dependency.** The convergence rate of a cavity decreases with increasing pore pressure. Assuming isotropic stress p_G in the surrounding rock, the dependency on the mean pore pressure \hat{p} is described by a factor

$$f_p = \left(1 - \frac{\hat{p} - p_{\text{ref}}}{p_G - p_{\text{ref}}}\right)^{m_p} \quad \text{for } p \leq p_G, \quad \text{otherwise } f_p = 0. \quad (5.4)$$

p_G is the isotropic lithostatic pressure that would have been present at the reference location in the absence of a cavity. The mean pore pressure \hat{p} is calculated as the

arithmetic mean of gas pressure p_{gas} and liquid pressure p_{liq} weighted by the liquid saturation S_{liq} in the following way.

$$\hat{p} = p_{\text{gas}}(1 - S_{\text{liq}}) + p_{\text{liq}}S_{\text{liq}} = p_{\text{gas}} + p_{\text{cap}}S_{\text{liq}} \quad (5.5)$$

Note that the variation of p_G with depth is not covered by this approach.

- **Backfill support.** The supporting pressure on the cavity walls caused by the backfill increases with increasing compaction. The factor

$$f_{\phi}(\phi, \phi_r) = \left[1 + \frac{h(\phi, \phi_r)}{(\phi \cdot g(\phi, \phi_r))^{1/m_{\phi}}} \right]^{-m_{\phi}} \quad \text{for } \phi < \phi_r, \text{ otherwise } f_{\phi} = 1, \quad (5.6)$$

describes the influence of the supporting pressure on the convergence rate, where ϕ_r is the porosity at the onset of the supporting pressure. Functions $h(\phi, \phi_r)$ and $g(\phi, \phi_r)$ are approximated by

$$h(\phi, \phi_r) = h_0 + h_1 \frac{\phi}{\phi_r} + h_2 \left(\frac{\phi}{\phi_r} \right)^2 + h_3 \left(\frac{\phi}{\phi_r} \right)^3 \quad \text{and} \quad (5.7)$$

$$g(\phi, \phi_r) = g_0 + g_1 \frac{\phi}{\phi_r} + g_2 \left(\frac{\phi}{\phi_r} \right)^2 \quad (5.8)$$

with $h_0 = 1$, $h_2 = -(3 + 2h_1)$, $h_3 = h_1 + 2$ and $g_0 = 1$. Parameters ϕ_0 , h_1 , g_1 , and g_2 are input parameters. Presently, we set $m_{\phi} = m_p$.

- **Transient processes.** After excavation, the convergence rate of an open cavity converges against a stationary convergence rate, namely against the reference convergence rate K_{ref} . The gradual transition to the stationary convergence rate is expressed by the factor f_t

$$f_t = 1 + \frac{1}{1 + \lambda_s^{-1} \ln(V_0/V)} \left(\frac{K_0}{K_{\text{ref}} \cdot f_{\phi}(\phi_0)} - 1 \right). \quad (5.9)$$

K_0 and ϕ_0 are the initial convergence rate and initial porosity, respectively, at the start of the simulation. Parameter λ_s chiefly depends on time and has to be determined by geomechanical calculations. For more details see /NOS 05/ and /NAV 13c/.

- **Temperature dependency.** Temperature has a strong influence on salt creep and thus on the convergence rate. Temperature dependency is captured by the factor

$$f_T(T) = \frac{1}{1+a} \cdot \exp\left(\frac{Q_1}{R} \cdot \left(\frac{1}{T_{\text{ref}}} - \frac{1}{T}\right)\right) + \frac{a}{1+a} \cdot \exp\left(\frac{Q_2}{R} \cdot \left(\frac{1}{T_{\text{ref}}} - \frac{1}{T}\right)\right). \quad (5.10)$$

The equation considers two creep processes with activation energies of Q_1 and Q_2 and a weighting parameter a . Variable T_{ref} is the reference temperature, that is to say the temperature of the rock at the time of measuring the reference convergence rate. T is the present temperature of the rock and R the universal gas constant. The equation is only valid for a homogeneous distribution of temperature.

5.2 Note on the compaction of saturated media

The compaction process can cause numerical problems if a fully liquid-saturated medium is compacted under undrained or nearly undrained conditions and if the compressibility of the rock is low. Under these conditions, pressure may rise quickly and cause a drastic decrease of time step width.

5.3 Input data

The module introduces the new input data block COMP (see Tab. 5.1). Parameters have to be input separately for each material. However, modification of single elements is possible via the permeability modifier PM of data Block ELEME. Setting PM to a negative value disables compaction of the respective element. In the following calculations, the absolute value of PM is used as permeability modifier.

Up to TOUGH2-GRS version 1, functions for porosity-dependent permeabilities and capillary pressures had to be introduced by means of the COMP module. In order to achieve downward compatibility, these functions are still part of the COMP data block, but the respective entries (line 5 to 8) are overruled by the corresponding input data of data block RELA. For this reason, these functions are described in chapter 14.4.

Tab. 5.1 Input format of data block COMP

Line	Column	Content	Format	Unit	Description	Variable
1	1-5	"COMP"	A5		Keyword	
2	1-5	Material name	A5		Name of compacting material (as defined in ROCKS) In the following, M is the material index.	
3	1-10	K_{ref}	G10.4	sec^{-1}	Reference convergence rate	COMP_KREF (M)
	11-20	f_{loc}	G10.4	1	Local modification of the reference convergence rate	COMP_FLOC (M)
	21-30	p_G	G10.4	Pa	Lithostatic pressure at the location if no cavity would exist	COMP_PG (M)
	31-40	$m_p = m_\phi$	G10.4	1	Exponent for the calculation of f_p	COMP_M (M)
	41-50	ϕ_r	G10.4	1	Porosity at which backfill support commences	COMP_PHIref (M)
	51-60	h_1	G10.4	1	Parameter for the calculation of f_ϕ	COMP_H1 (M)
	61-70	g_1	G10.4	1	Parameter for the calculation of f_ϕ	COMP_G1 (M)
	71-80	g_2	G10.4	1	Parameter for the calculation of f_ϕ	COMP_G2 (M)
4	1-10	λ_s	G10.4	1	Parameter for the calculation of f_T	COMP_LAMBDA (M)
	11-20	K_0	G10.4	sec^{-1}	Initial convergence rate	COMP_K0 (M)
	21-30	a	G10.4	1	Weighting factor for creep processes	COMP_A (M)
	31-40	Q_1	G10.4	J/mol	Activation energy for creep process 1	COMP_Q1 (M)
	41-50	Q_2	G10.4	J/mol	Activation energy for creep process 2	COMP_Q2 (M)
	51-60	T_{ref}	G10.4	$^{\circ}C$	Temperature of the rock at the reference location	COMP_TGREF (M)
	61-70	ϕ_{lim}	G10.4	1	Lower porosity limit for the convergence process (may be 0)	COMP_PHIMIN (M)
5	1-10	0 or 1	I10	1	Enable Leverett scaling of capillary pressures? (0 = no, 1 = yes)	COMP_LEVQ (M)
	11-20	k_0	G10.4	m^2	Reference permeability for Leverett scaling	COMP_LEVPERREF (M)
	21-30	ϕ_0	G10.4	1	Reference porosity for Leverett scaling	COMP_LEVPHIREF (M)
	31-40	α	G10.4	1	Exponent of the Leverett scaling	COMP_LEVEXP (M)
6	1-10	$\phi_{k=0}$	G10.4	1	Permeability will be 0 for porosities $\leq \phi_{k=0}$	COMP_CUTOFF (M)
7	1-10	n_{sec}	I10	1	Number of subsections of the porosity-permeability relation	COMP_NBRANCH (M)
8	1-10	a_i	G10.4	m^2	Factor of power law i	COMP_PERA (I, M)
	11-20	b_i	G10.4	m^2	Exponent of power law i	COMP_PERB (I, M)
<i>Repeat line 8 for all n_{sec} sections</i>						
<i>Repeat line 2 to 7+n_{sec} for all compacting materials</i>						

6 CORFL

The CORFL module simulates permeability changes of technical barriers (seals) caused by percolating corrosive solutions. Although originally designed for the simulation of salt concrete corrosion by magnesium bearing solutions the module has no restrictions with regard to the underlying chemistry of the seal and percolate.

6.1 Implementation

The CORFL module uses the primary variable *brine mass fraction* to store information on the corrosion capacity of the fluid. The brine mass fraction of *normal corrosive brine* (this term will be defined below) and non-corrosive brine is specified by the input parameters \tilde{X}_b and \hat{X}_b . In the following we assume $\tilde{X}_b < \hat{X}_b$ indicating that the brine mass fraction increases during the corrosion process. However, the CORFL module also accepts $\tilde{X}_b > \hat{X}_b$.

If a corrosive fluid with brine mass fraction X_b enters a corrodible grid element, the CORFL module changes the composition of the brine to that of non-corrosive brine, that is to brine mass fraction \hat{X}_b . Thus, downstream elements are not corroded. The physical assumption behind this model is a quick corrosion process causing a sharp corrosion front.

In order to raise the brine mass fraction inside a corroding element from X_b to \hat{X}_b , the CORFL module places a brine source and a water sink at the grid element. The source and the sink are adjusted so that the change of brine composition is an isovolumetric process. This is necessary to maintain constant pore pressures during the corrosion process.

The cumulative brine mass that has been released from a seal element until time t determines its degree of corrosion. The degree of corrosion is 0 for non-corroded materials and 1 for full corrosion. The permeability of a material changes in response to its degree of corrosion.

6.2 Source and sink calculation

The introduced brine sources and water sinks are corrected in every Newton-Raphson iteration. If the brine inside a corroding element has a brine mass fraction of $X_b \neq \hat{X}_b$ the brine source and water sink of that element must be adapted in order to achieve $X_b = \hat{X}_b$. The method for doing so is to first calculate the brine and water mass that should be present at $X_b = \hat{X}_b$ and then to add or subtract the missing or excessive masses to the source and sink. If m_b is the brine mass of the current Newton-Iteration and \hat{m}_b the brine mass required for $X_b = \hat{X}_b$, the brine source is corrected in this Newton-Iteration by adding the term

$$\frac{\hat{m}_b - m_b}{V \Delta t} \quad (6.1)$$

where V is the element volume and Δt is the time step. The current brine mass m_b can be calculated from the secondary variables (`PAR` array) of TOUGH2

$$m_b = V \cdot \phi \cdot S_1 \cdot \rho_1(X_b) \cdot X_b \quad (6.2)$$

with porosity ϕ , liquid saturation S_1 , liquid density ρ_1 , and the current brine mass fraction X_b .

Since the change of brine mass fraction must not affect the liquid volume, the product $V \cdot \phi \cdot S_1$ has to remain constant. The intended brine mass

$$\hat{m}_b = V \cdot \phi \cdot S_1 \cdot \rho_1(\hat{X}_b) \cdot \hat{X}_b \quad (6.3)$$

therefore refers to $V \cdot \phi \cdot S_1$ with $\rho_1(\hat{X}_b)$ being the liquid density at $X_b = \hat{X}_b$. Liquid density $\rho_1(\hat{X}_b)$ can be calculated using the formula implemented in the equation-of-state modules EOS7 and EOS7R, which refers to the density of pure water ρ_w :

$$\rho_1(X_b) = \frac{\rho_w d}{d(1 - X_b) + X_b} \quad (6.4)$$

with

$$d = \frac{\rho_b(p_0, T_0)}{\rho_w(p_0, T_0)} \quad (6.5)$$

being the ratio between the density of the reference brine ρ_b and the density of pure water ρ_w at reference conditions p_0 and T_0 .

To avoid calculating the density of pure water, ρ_w is substituted by applying equation (6.4) to the brine densities \hat{X}_b and X_b

$$\rho_l(\hat{X}_b) = \rho_l(X_b) \frac{1 - X_b + \frac{X_b}{d}}{1 - \hat{X}_b + \frac{\hat{X}_b}{d}}. \quad (6.6)$$

Combining this equation with equation (6.3) allows to calculate the intended brine mass by means of the given primary and secondary variables of TOUGH2:

$$\hat{m}_b = V \phi S_l \rho_{liq}(X_b) \frac{1 - X_b + \frac{X_b}{d}}{1 - \hat{X}_b + \frac{\hat{X}_b}{d}} \hat{X}_b. \quad (6.7)$$

The same procedure is used to calculate the intended water mass

$$\hat{m}_w = V \cdot \phi \cdot S_l \cdot \rho_l(\hat{X}_b) \cdot (1 - \hat{X}_b), \quad (6.8)$$

which leads to

$$\hat{m}_w = V \phi S_l \rho_{liq}(X_b) \frac{1 - X_b + \frac{X_b}{d}}{1 - \hat{X}_b + \frac{\hat{X}_b}{d}} (1 - \hat{X}_b). \quad (6.9)$$

6.3 Degree of corrosion

The *corrosion potential* γ is defined as the ratio between the volume of corroded solid and the liquid volume necessary for its complete corrosion. In our model, the reference liquid for the definition of the corrosion potential is a liquid, which we call which we call *normal corrosive brine* and which is characterized by a brine mass fraction of \hat{X}_b .

If V is the volume of a grid element and ϕ its porosity, $V(1 - \phi)$ is the solid volume and $V\phi$ the pore volume. If full liquid saturation is considered, we obtain the number of times the pore fluid must be exchanged for complete corrosion by

$$n = \frac{V(1 - \phi)}{V\phi \gamma}. \quad (6.10)$$

Corrosion takes place if corrosive liquid with brine mass fraction \tilde{X}_b and brine mass m_b infiltrates. Raising the brine mass fraction from \tilde{X}_b to \hat{X}_b (and brine mass from m_b to \hat{m}_b) a brine mass of $\hat{m}_b - m_b$ has to be injected. Equation (6.9) shows that a complete corrosion of the solid requires a brine mass injection of

$$m_{b,\max} = n(\hat{m}_b - m_b) = nV\phi S_1 \rho_1(\tilde{X}_b) \left(\frac{1 - \tilde{X}_b + \frac{\tilde{X}_b}{d}}{1 - \hat{X}_b + \frac{\hat{X}_b}{d}} \hat{X}_b - \tilde{X}_b \right). \quad (6.11)$$

If $m_{b,\text{sum}}(t)$ is the brine mass released by a brine source until time t , the degree of corrosion $g(t)$ of the grid element is

$$g(t) = \frac{m_{b,\text{sum}}}{m_{b,\max}}. \quad (6.12)$$

6.4 Permeability change

We adopt the physical model of /BFS 09/ (p. 154 ff) for the permeability change of corroding seals. The model assumes a sharp, planar corrosion front migrating through the grid element due to a homogenous percolation of the seal. The corrosion front separates fully corroded material from material without any corrosion. Kinetic effects that could smoothen out the corrosion front are neglected. Note that this model might not capture the true physics of seal corrosion for all types of seals especially if seal percolation and corrosion are highly localized.

Due to the assumption of a sharp corrosion front, the degree of corrosion g denotes the corroded fraction of a grid element. We keep permeability unchanged if $g = 0$. In case of $g = 1$, permeability is multiplied by a factor of 10^{ε_k} . For a partly corroded material we assume a series connection of corroded and non-corroded material which yields

$$f_{\text{CORFL}} = \frac{1}{1 - g(1 - 10^{-\varepsilon_k})} \quad (6.13)$$

for the permeability modifier f_{CORFL} . See chapter 2.7 for details on how f_{CORFL} is used to modify the intrinsic permeability of a grid element.

6.5 Input data

Tab. 6.1 summarizes the input parameters of the CORFL module. All corrosion parameters are material-specific.

Tab. 6.1 Input format of data block CORFL

Line	Column	Content	Format	Unit	Description	Variable	
1	1-5	"CORFL"	A5		Keyword		
2	1-5	material name	A5		Name of compacting material (as defined in ROCKS) In the following, M is the material index.		
3	1-10	γ	G10.4	1	Corrosion potential (volume of solid corroded per solute volume)	CORFL_UK (M)	
	11-20	<i>unused</i>					
	21-30	\bar{X}_b	G10.4	1	Brine mass fraction of corrosive brine (choose brine used in corrosion experiment in order to determine corrosion potential)	CORFL_XB1 (M)	
	31-40	\hat{X}_b	G10.4	1	Brine mass fraction of non-corrosive brine (choose $\hat{X}_b \neq \bar{X}_b$)	CORFL_XB2 (M)	
	41-50	<i>unused</i>					
	51-60	ε_k	G10.4	1	Permeability factor of fully corroded element is 10^{ε_k}	CORFL_EK (M)	
<i>Repeat line 2 to 3 for all corroding materials</i>							

7 CORRO: Gas production due to iron corrosion

In repositories for radioactive waste, corrosion of iron is an important gas source. Iron corrosion requires the presence of water and consequently that the availability of water can become a limiting factor for gas production. Water-dependent iron corrosion can be simulated by the CORRO module by introducing gas sources and liquid sinks.

Gas sources are characterized by a gas generation rate (mole per second) and a maximum amount of produced gas. Gas sources can be either placed inside a grid element or distributed over a material domain assuming equal gas generation rate per element volume within the domain.

Gas sources can be specified as water consuming sources. In this case, gas production is limited to the availability of water. The rate of water consumption is coupled to the rate of gas production by the ratio $r_{w/g}$ (CORRO_moleWaterPerMoleGas), which describes how many mole of water are consumed for every mole of gas that is produced.

Each gas source becomes inactive as soon as the maximum amount of gas has been produced. The current *degree of corrosion* is the fraction of the maximum amount of gas produced at a certain time.

7.1 Water consumption

The COMP module offers three sources for water consumption:

1. the water contained in wastes and waste packages,
2. the water component of the liquid phase, and
3. the water implicitly contained in the brine component of the liquid phase.

The water mass contained in wastes and waste packages is input via parameter m_{can} . This water does not participate in the flow system. It is solely amenable to the corrosion process and consumed prior to the pore water.

Liquid consumption begins with the disappearance of canister water. The water component of the liquid is consumed first followed by the consumption of the brine component. The consumption rate for the brine component is higher than for the water com-

ponent since brine is not completely composed of water. Input parameter $r_{w/b}$ (`CORRO_waterMassPerBrineMass`) determines the mass of water that is implicitly contained in a liquid with brine mass fraction 1.

Water consumption is enabled by setting `CORRO_consumeWater` to 1 and disabled by default. Canister water is always available for corrosion if water consumption has been enabled. Pore water consumption has to be enabled separately by setting parameter `CORRO_consumePoreWater` to 1. Pore water is unavailable for the corrosion process if liquid saturation falls below the saturation limit S_{empty}^{CORRO} (`CORRO_Sliqempty`).

7.2 Gas component

The CORRO module requires the equation-of-state modules EOS7 and EOS7R and generates the non-condensable gas component of these EOS modules.

For reasons of simplicity we assume that gas is able to escape from the canister immediately, for example, because of pitting corrosion. The CORRO module therefore does not distinguish between gas produced inside and outside the waste canisters. The user should be aware that this assumption can be inadequate for some physical problems.

The main gas component of chemical iron corrosion is hydrogen but the non-condensable gas produced by EOS7 and EOS7R is air. If hydrogen should be the main gas component in the simulation, the properties of the gas component can be changed by means of the GCOMP module (see chapter 13).

Changing the gas component via GCOMP may be insufficient if the gas composition changes with time or location. The user should therefore reflect on possible errors resulting from the choice of a gas component that does not represent the gas component of the real system. Erroneous viscosity of the vapour-gas mixture causes errors in the gas flow. This should be corrected by choosing an appropriate viscosity function by means of the GCOMP module. A wrong atomic weight leads to errors in gas density as well as in the mass and mass fraction of the gas component. However, an erroneous atomic weight does not necessarily cause an erroneous transport of gas in terms of amount of substance. This has the following reasons.

- For a given amount of substance of a gas component, gas pressure is independent of atomic weight because of the implemented ideal gas law.
- Atomic weight has no major impact on liquid density if the mass fraction of dissolved gas is small (which usually is the case).
- According to Henry's law, the partial pressure of the main gas component is proportional to the mole fraction of the dissolved component. For this reason the amount of gas dissolved in liquid is independent of the gas component's atomic weight.
- The effect of the atomic weight on the diffusion of gas in the liquid phase is negligible. Let κ be the gas component of TOUGH2-GRS and $\hat{\kappa}$ the real gas component. If the dissolved amount of gas is equal for both gas components (i. e. $n^\kappa = n^{\hat{\kappa}}$) and if we set the diffusion coefficient of component κ equal to that of component $\hat{\kappa}$, i. e.

$$d_{\text{liq}}^\kappa := d_{\text{liq}}^{\hat{\kappa}}, \quad (7.1)$$

the diffusive flux of component κ in the liquid phase is equal to that of the real component $\hat{\kappa}$ in terms of the amount of substance:

$$\frac{f_{\text{liq}}^{\hat{\kappa}}}{\mu_{\hat{\kappa}}} = \frac{f_{\text{liq}}^\kappa}{\mu_\kappa} \quad (7.2)$$

with f_β^κ being the diffusive mass flow in phase β and μ_κ the atomic weight of component κ . Equation (7.2) is derived by substituting the diffusive mass flows with the corresponding TOUGH2 equation

$$f_\beta^\kappa = -\phi\tau_0\tau_\beta\rho_\beta d_\beta^\kappa \nabla X_\beta^\kappa. \quad (7.3)$$

This gives

$$m_{\text{liq}} d_{\text{liq}}^\kappa \nabla \frac{n^\kappa}{m_{\text{liq}}} = \hat{m}_{\text{liq}} d_{\text{liq}}^{\hat{\kappa}} \nabla \frac{n^{\hat{\kappa}}}{\hat{m}_{\text{liq}}}$$

which again reduces to equation (7.1) under the approximation that dissolved gases only have little influence on liquid density and that liquid density is constant in space.

- The same operations applied to the diffusion in the gas phase lead to

$$m_{\text{gas}} d_{\text{gas}}^\kappa \nabla \frac{n^\kappa}{m_{\text{gas}}} = \hat{m}_{\text{gas}} d_{\text{gas}}^{\hat{\kappa}} \nabla \frac{n^{\hat{\kappa}}}{\hat{m}_{\text{gas}}}. \quad (7.4)$$

Gas masses m_{gas} and \hat{m}_{gas} depend on the atomic weights so that equation (7.3) reduces to

$$d_{\text{gas}}^{\kappa} = d_{\text{gas}}^{\hat{\kappa}} \quad (7.5)$$

only if either vapour or the main gas component is absent. Diffusion in the gas phase may therefore be affected by errors in atomic weight.

The user should therefore specify gas sources in terms of the amount of substance. The interpretation of the simulated gas transport should also focus on the amount of substance.

7.3 Gas generation rates

Each gas source is specified by the maximum amount of producible gas N_{tot} (CORRO_moleGas) and a gas generation rate Q . Corrosion experiments usually consider the rate of gas generation as a function of time t . We therefore use time-dependent rate functions to specify gas generation rates.

Corrosion at full liquid saturation

The CORRO module offers an exponential and a power law relationship to describe the corrosion rates for full liquid saturation (i. e. the entire gas source is in contact with water). The exponential function

$$Q_e(t) = A_{\text{liq}} e^{Bt} \quad , B < 0, \quad (7.6)$$

where A_{liq} and B are fitting parameters, is selected by `usePowerLaw=0`. The power law relationship

$$Q_p(t) = a \left(\frac{t-t_0}{t_{\text{ref}}} \right)^n \quad , n < 0 \quad \text{and} \quad t - t_0 \neq 0 \quad (7.7)$$

is selected by `usePowerLaw = 1`. Parameters a , t_0 , t_{ref} , and n are fitting parameters.

The amount of gas produced until time t is

$$N(t) = \int_{\hat{t}=0}^t Q(\hat{t}) d\hat{t}. \quad (7.8)$$

Using equations (7.6) and (7.7) for Q leads to

$$N(t) = \frac{A_{\text{liq}}}{B} (e^{Bt} - 1) \quad (7.9)$$

for the exponential function and

$$N(t) = \begin{cases} \frac{a t_{\text{ref}}}{n+1} \left[\left(\frac{t-t_0}{t_{\text{ref}}} \right)^{n+1} - \left(\frac{t_0}{t_{\text{ref}}} \right)^{n+1} \right] & \text{for } n \neq -1 \\ a t_{\text{ref}} \ln \left(1 + \frac{t}{t_0} \right) & \text{for } n = -1 \end{cases} \quad (7.10)$$

for the power law function.

Equations (7.6) and (7.7) are not implemented directly because time-discretization of production rates would lead to a rough approximation of the cumulative amount of produced gas according to equation (7.8). Instead, the mean production rate \bar{Q} of time step Δt is calculated by

$$\bar{Q}_{t_{\text{old}} \rightarrow t_{\text{old}} + \Delta t} := \frac{N(t_{\text{old}} + \Delta t) - N(t_{\text{old}})}{\Delta t}, \quad (7.11)$$

with starting time t_{old} is. \bar{Q} is the production rate under full liquid saturation. The production rate for limited water availability \tilde{Q} will be derived from \bar{Q} further below.

In order to calculate \bar{Q} we need the amount of gas that had been produced at the last time step $N(t_{\text{old}})$. TOUGH2-GRS does not store $N(t_{\text{old}})$ but it stores the normalized value of $N(t_{\text{old}})$, which we call the *degree of corrosion*

$$g(t) := \begin{cases} \frac{N(t)}{N_{\text{tot}}} & \text{if less than 1} \\ 1 & \text{otherwise} \end{cases}. \quad (7.12)$$

N_{tot} is the total amount of gas that can be produced by the source (an input parameter). Using the degree of corrosion, equation (7.11) can be rewritten as

$$\bar{Q}_{t_{\text{old}} \rightarrow t_{\text{old}} + \Delta t} := \frac{N(t_{\text{old}} + \Delta t) - g(t_{\text{old}}) N_{\text{tot}}}{\Delta t}. \quad (7.13)$$

Corrosion with limited water availability

Up to now, Q and N have been functions of time. To allow for a temporal stagnancy of corrosion, equation (7.13) is generalized by describing the time variable of rate function Q as a function of the degree of corrosion

$$\theta: g \mapsto t \quad (7.14)$$

so that we receive

$$\bar{Q}_{t_{\text{old}} \rightarrow t_{\text{old}} + \Delta t} = \frac{N(\theta(g(t_{\text{old}})) + \Delta t) - g(t_{\text{old}}) N_{\text{tot}}}{\Delta t}. \quad (7.15)$$

The time function θ is derived by solving equation (7.12) with the help of equation (7.9) or (7.10), which gives us

$$\theta(g) = \frac{1}{B} \ln \left(\frac{gN_{\text{tot}}B}{A_{\text{liq}}} + 1 \right) \quad (7.16)$$

for the exponential function and

$$\theta(g) = \begin{cases} \left[\frac{gN_{\text{tot}}(n+1)}{t_{\text{ref}} a} - \left(\frac{t_0}{t_{\text{ref}}} \right)^{n+1} \right]^{\frac{1}{n+1}} t_{\text{ref}} - t_0 & \text{for } n \neq -1 \\ t_0 \left(\exp \frac{gN_{\text{tot}}}{t_{\text{ref}} a} - 1 \right) & \text{for } n = -1 \end{cases} \quad (7.17)$$

for the power law function.

Equations (7.16) and (7.17) are only used if `dependsOnTime=0`. Otherwise, the function $\theta(g) = t_{\text{old}}$ is used meaning that the corrosion rate decreases with time even if the corrosion process is stalled. The user should be aware that this usually is not a reasonable physical behaviour.

The production rate for limited water availability \tilde{Q} is used as production rate for unlimited water supply \bar{Q} unless water consumption is enabled (`CORRO_consumeWater=1`) and corrosion rates depend on the degree of corrosion (`corro_dependsOnTime=0`). In the following we consider the opposite case with $\tilde{Q} \neq \bar{Q}$.

If water consumption is enabled and corrosion rates depend on the degree of corrosion, the production rate for limited water availability \tilde{Q} depends on how the switch `CORRO_AssumeWaterTable` is set. The switch decides which fraction of the gas source is in contact with water under unsaturated conditions. If the capillary fringe is small compared to the height of a grid element, we can assume the formation of a horizontal water table. Under these circumstances the element's liquid saturation can be viewed as the fraction α of the element that is below the water table, that is to say under full liquid saturation. Choosing `CORRO_AssumeWaterTable=1` sets $\alpha = S_{\text{liq}}$. In all other cases α is equal to 1.

If there is a water table, we define

$$\tilde{Q}_{t_{\text{old}} \rightarrow t_{\text{old}} + \Delta t} := \frac{\alpha A_{\text{liq}} e^{Bt} + (1 - \alpha) A_{\text{vap}}}{A_{\text{liq}}} \bar{Q}_{t_{\text{old}} \rightarrow t_{\text{old}} + \Delta t} \quad (7.18)$$

for the exponential function and

$$\tilde{Q}_{t_{\text{old}} \rightarrow t_{\text{old}} + \Delta t} := \alpha \bar{Q}_{t_{\text{old}} \rightarrow t_{\text{old}} + \Delta t} \quad (7.19)$$

for the power law function.

7.4 Input data

Tab. 7.1 shows the input parameters of data block CORRO.

Tab. 7.1 Input format of data block CORRO

Line	Column	Content	Format	Unit	Description	Variable
1	1-5	"CORRO"	A5		Keyword	
2	1-10	$R_{w/b}$	G10.4	–	Water mass per brine mass Default: 0.46	CORRO_waterMassPer-BrineMass
2	11-20	S_{empty}^{CORRO}	G10.4	–	Pore water consumption only if $S_{liq} > S_{empty}^{CORRO}$	CORRO_Sliqempty
3	1-5	"E", "e", "M", "m"	A5		Location type. Gas source is either placed in an element ("E", "e") or homogeneously distributed over a material ("M", "m").	CORRO_loctype(s) s is the source index
3	6-10	Location	A5		Element or material name	CORRO_loc(s)
3	11-15	Switch: consume water?	I5	1	Stop gas generation in absence of water? 0: no, 1: yes	CORRO_consumeWater(s)
3	16-20	Switch: consume pore water?	I5	1	Stop gas generation in absence of pore water? 0: no, 1: yes	CORRO_consumePoreWater(s)
3	21-25	Switch: Assume water table?	I5	1	Recognize liquid saturation as relative height of a water table inside an element? 0: no, 1: yes	CORRO_assumeWaterTable(s)
3	26-30	Switch: Use time-dependent rate function?	I5	1	Calculate generation rates using the time instead of the degree of corrosion? 0: no, 1: yes	CORRO_dependsOnTime(s)
3	31-40	A_{liq}	G10.4	mol/s	Fitting parameter of exponential rate function for water contact	CORRO_Aliquid(s)
3	41-50	A_{vap}	G10.4	mol/s	Fitting parameter of exponential rate function for vapour contact	CORRO_Avapour(s)
3	51-60	B	G10.4	1/s	Fitting parameter of exponential rate function. 0: constant rate, <0: decreasing rate	CORRO_B(s)
3	61-70	–	–	–	INACTIVE	–
3	71-80	Switch: Use power function?	G10.4		Use power function instead of exponential function? 0: no, 1: yes	CORRO_useFunction2(s)
4	1-10	g_0	G10.4	1	Initial degree of corrosion	CORRO_initialDegreeOfCorrosion(s)
4	11-20	N_{tot}	G10.4	mol	Maximum amount of gas that can be produced	CORRO_moleGas(s)
4	21-30	m_{can}	G10.4	kg	Canister water	CORRO_canisterWaterMass(s)
4	31-40	$r_{w/g}$	G10.4	1	Mole of water consumed for every mole of gas that is produced	CORRO_moleWaterPerMoleGas(s)
4	41-50	a	G10.4	mol/s	Fitting parameter of power law rate function	CORRO_f2_a(s)
4	51-60	n	G10.4	1	Fitting parameter of power law rate function	CORRO_f2_n(s)
4	61-70	t_0	G10.4	s	Fitting parameter of power law rate function	CORRO_f2_t0(s)
4	71-80	t_{ref}	G10.4	s	Fitting parameter of power law rate function	CORRO_f2_tref(s)
<i>Repeat lines 3 and 4 for all gas sources</i>						

8 DEGRA: Time-dependent permeability changes

8.1 Model and implementation

The main function of technical seals is to prevent fluid flow. There are many physical and chemical processes contributing to seal degradation which is why a general-purpose module for the simulation of seal degradation must be very general and simple. Based on these considerations the DEGRA module introduces seal degradation as a time-dependent change of permeability. Intrinsic permeability is changed by means of a permeability modifier f_{DEGRA} (see chapter 2.7). Degradation takes place in a user-defined time window $[t_1, t_2]$ in which f_{DEGRA} increases linearly from 1 to the target value F :

$$f_{\text{DEGRA}} = \begin{cases} 1 & \text{for } t \leq t_1 \\ 1 + \left(\frac{t - t_1}{t_2 - t_1} \right) (F - 1) & \text{for } t_1 < t < t_2 \\ F & \text{for } t \geq t_2 \end{cases} \quad (8.1)$$

8.2 Input data

Tab. 8.1 shows the input data block of the DEGRA module.

Tab. 8.1 Input format of data block DEGRA

Line	Column	Content	Format	Unit	Description	Variable
1	1-5	"DEGRA"	A5		Keyword	
2	1-5	material name	A5		Name of degrading material (as defined in ROCKS). In the following, M is the material index.	
2	6-15	t_1	G10.4	sec	Start time of permeability change t_1	DEGRA_T1 (M)
2	16-25	t_2	G10.4	sec	End time of permeability change t_2	DEGRA_T2 (M)
2	26-35	F	G10.4	1	Factor F for the permeability at the time t_2	DEGRA_F (M)
<i>Repeat line 2 for required materials</i>						

9 DOFT

DOFT is a new data block for domain-specific time series. It complements the existing data blocks FOFT, COFT, and GOFT, which are element-, connection-, and source-specific. Attention has to be paid with regard to the numbering of materials in the generated output file DOFT. Material 1 of the DOFT output file refers to entire model system excluding inactive elements. Since this domain is not (and cannot be) specified in the input data block, the first material of the DOFT input data block refers to the second material in the DOFT output file and so on. The content of the DOFT output file is described in chapter 0.

Tab. 9.1 Input format of data block DOFT

Line	Column	Content	Format	Unit	Variable
1	1-5	Keyword "DOFT"	A5		
2	1-5	Material	A5	[1]	edoft

Repeat line 2 for all required materials. Material 1 will be the second material index in the DOFT file, because the first index is reserved for the entire model domain.

10 FISS: Gas pathway dilation

The transport of gas in low-permeability host rock, like clay stone or rock salt, becomes more efficient at high gas pressures. The increase of transport efficiency is not a gradual process but one that is controlled by pressure thresholds due to the opening of microscopic pathways, a process often referred to as “pathway dilation”. At even higher pressures, macroscopic fracturing may take place.

The FISS module introduces several models for threshold-driven advective gas transport. Models for the change of pressure thresholds (softening), porosity, and gas permeability can be combined.

The FISS module makes use of the porosity change mechanism explained earlier in chapter 2.6. Changes of gas permeability do not affect intrinsic permeability but are introduced by adding a new permeability term to the flow equation for the gas phase. This is explained in chapter 10.3.

10.1 Pressure thresholds and softening models

We introduce a threshold pressure for the gas flow in dilating micro-fissures p_{thr} . The term softening will be used for a decrease of the threshold pressure. The decrease that takes place between successive time steps is denoted by Δp_{thr} and it is controlled by a softening model that can be selected and specified by use of input parameters `ifsoft` and `fsoft` (see Tab. 10.1). The softening model `ifsoft` quantifies the change of threshold pressure $\widetilde{\Delta p}_{\text{thr}}$ required for an instantaneous equilibration of pressure and threshold pressure. Parameter `fsoft(3)` specifies how the value of $\widetilde{\Delta p}_{\text{thr}}$ is approached by the actual pressure change Δp_{thr} with time.

Equilibrium model

- `ifsoft=0`: Constant threshold, no softening.

$$\widetilde{\Delta p}_{\text{thr}} = 0 \tag{10.1}$$

- `ifsoft=1`: Reversible linear softening.

The threshold pressure p_{thr} decreases linearly from $p_{\text{thr,ini}}$ to $p_{\text{thr,ini}} - f_{\text{soft}}(2)$ as p increases from $p_{\text{thr,ini}}$ to $p_{\text{thr,ini}} + f_{\text{soft}}(1)$.

$$\widetilde{\Delta p}_{\text{thr}} = \begin{cases} -p_{\text{thr}} + p_{\text{thr,ini}} & \text{for } x_{\text{thr}} < 0 \\ -p_{\text{thr}} - x_{\text{thr}} \cdot f_{\text{soft}}(2) + p_{\text{thr,ini}} & \text{for } 0 \leq x_{\text{thr}} \leq 1 \\ -p_{\text{thr}} - f_{\text{soft}}(2) + p_{\text{thr,ini}} & \text{for } x_{\text{thr}} > 1 \end{cases} \quad (10.2)$$

with

$$x_{\text{thr}} = \frac{p - p_{\text{thr,ini}}}{f_{\text{soft}}(1)}. \quad (10.3)$$

- $f_{\text{soft}}=2$: Irreversible linear softening. Same as $f_{\text{soft}}=2$ but positive values of $\widetilde{\Delta p}_{\text{thr}}$ are clipped to zero.

Time-dependency models

- $f_{\text{soft}}(3)=0$: No time-dependency,

$$\Delta p_{\text{thr}} = \widetilde{\Delta p}_{\text{thr}}. \quad (10.4)$$

- $f_{\text{soft}}(3)=1$: Positive rate limit $f_{\text{soft}}(4)$,

$$\Delta p_{\text{thr}} = \min(|\widetilde{\Delta p}_{\text{thr}}|, f_{\text{soft}}(4) \Delta t) \text{sgn}(\widetilde{\Delta p}_{\text{thr}}). \quad (10.5)$$

- $f_{\text{soft}}(3)=2$: Rate decrease according to a decay function with half-life $f_{\text{soft}}(4)$,

$$\Delta p_{\text{thr}} = \widetilde{\Delta p}_{\text{thr}} \left(1 - 2^{-\frac{\Delta t}{f_{\text{soft}}(4)}} \right). \quad (10.6)$$

10.2 Fissure porosity models

Similar relations are used for fissure porosity. Parameter f_{por} selects a model for the change of fissure porosity $\widetilde{\Delta \phi}_{\text{fiss}}$ due to instantaneous equilibration. The actual change of fissure porosity $\Delta \phi_{\text{fiss}}$ approaches $\widetilde{\Delta \phi}_{\text{fiss}}$ according to time-dependency effects selected by parameter $f_{\text{por}}(\text{matno}, 5)$.

Equilibrium models

- $f_{\text{por}}=0$: No porosity change.

$$\widetilde{\Delta \phi}_{\text{fiss}} = 0 \quad (10.7)$$

- $f_{\text{por}}=1$: Porosity switches between two values. This model should only be used in combination with a kinetic model in order to avoid oscillations.

$$\widetilde{\Delta\phi}_{\text{fiss}} = \begin{cases} f_{\text{por}}(1) - \phi_{\text{fiss}} & \text{for } p > p_{\text{thr}} \\ -\phi_{\text{fiss}} & \text{for } p \leq p_{\text{thr}} \end{cases} \quad (10.8)$$

- $f_{\text{por}}=2$: Power-law behaviour with optional cut-off.

$$\widetilde{\Delta\phi}_{\text{fiss}} = \begin{cases} -\phi_{\text{fiss}} + f_{\text{por}}(2) & \text{for } p > p_{\text{thr}} \wedge f_{\text{por}}(4) = 1 \\ -\phi_{\text{fiss}} + f_{\text{por}}(2) (x_{\text{por}})^{f_{\text{por}}(3)} & \text{for } p > p_{\text{thr}} \wedge f_{\text{por}}(4) \neq 1, \\ -\phi_{\text{fiss}} & \text{for } p \leq p_{\text{thr}} \end{cases} \quad (10.9)$$

with

$$x_{\text{por}} = \frac{p - p_{\text{thr}}}{f_{\text{por}}(1)}. \quad (10.10)$$

Time-dependency models

- $f_{\text{por}}(\text{matno}, 5)=0$: No time-dependency.

$$\Delta\phi_{\text{fiss}} = \widetilde{\Delta\phi}_{\text{fiss}}. \quad (10.11)$$

- $f_{\text{por}}(\text{matno}, 5)=1$: Positive rate limit $f_{\text{por}}(6)$.

$$\Delta\phi_{\text{fiss}} = \min(|\widetilde{\Delta\phi}_{\text{fiss}}|, f_{\text{por}}(6) \Delta t) \text{sgn}(\widetilde{\Delta\phi}_{\text{fiss}}). \quad (10.12)$$

- $f_{\text{por}}(\text{matno}, 5)=2$: rate decrease according to an exponential decay function with half-life b_6 .

$$\Delta\phi_{\text{fiss}} = \widetilde{\Delta\phi}_{\text{fiss}} \left(1 - 2^{-\frac{\Delta t}{f_{\text{por}}(6)}} \right). \quad (10.13)$$

10.3 Permeability models

The flow equation for the gas phase is extended by an additional term $k_{\text{dil}}\mathbf{K}_{\text{dil}}$ for the flow through fissures.

$$F_{\text{gas}} = -\frac{\rho_{\text{gas}}}{\mu_{\text{gas}}} \left(k_{r,\text{gas}} \mathbf{I} + \underbrace{k_{\text{dil}} \mathbf{K}_{\text{dil}}}_{\text{micro crack permeability}} \right) (\nabla p_{\text{gas}} - \rho_{\text{gas}} \mathbf{g}) \quad (10.14)$$

k is the intrinsic permeability, $k_{r, \text{gas}}$ relative gas permeability, ρ_{gas} gas density, μ_{gas} the dynamic viscosity of the gas phase, and g the vector of gravitational acceleration. Variable k_{dil} is the pressure-dependent gas permeability of the fissure network, and tensor $\mathbf{K}_{\text{dil},i}$ (input parameter `fiss_tensor`) introduces anisotropy.

It is assumed that micro cracks already opened by an intruding gas phase remain unsaturated, and for this reason no relative gas permeability is introduced for the micro crack network.

The two terms in the large brackets of equation (10.14) stand for the permeability of the original pore space and that of the secondary pore space created by pathway dilation. In the space-discretised version of equation (10.14), these two terms are weighted separately with $k_{\text{dil}}\mathbf{K}_{\text{dil}}$ always being upstream-weighted.

k_{dil} is defined as a power function with lower and optional upper cut-off

$$k_{\text{dil}} = \begin{cases} \text{fper}(3) & y < 0 \\ \text{fper}(4) & y > 1 \wedge \text{fper}(6) \neq 0 \\ y^{\text{fper}(5)} \cdot (\text{fper}(4) - \text{fper}(3)) + \text{fper}(3) & \text{otherwise} \end{cases} \quad (10.15)$$

with

$$y = \frac{x - \text{fper}(1)}{\text{fper}(2) - \text{fper}(1)}. \quad (10.16)$$

Parameter `fper(6)` introduces an upper cutoff of k_{dil} . The meaning of x , `fper(1)`, and `fper(2)` depends on the choice of `ifper`:

- `ifper=0`: $x = \text{fper}(1)$ (constant permeability $k_{\text{dil}} = \text{fper}(3)$)
- `ifper=1`: $x = \phi_{\text{fiss}}$ (k_{dil} is a function of fissure porosity)
- `ifper=2`: $x = p - p_{\text{thr}}$ (k_{dil} is a function of gas pressure)
- `ifper=3`: $x = p_{\text{thr}}$ (k_{dil} is a function of the pressure threshold)

10.4 Input data

Tab. 6.1 shows the parameters of input data block FISS. Micro-fissuring is activated for materials.

Tab. 10.1 Input format of data block FISS

Line	Column	Content	Format	Unit	Description	Variable
1	1-5	"FISS"	A5		Keyword	
2	1-5	Material name	A5		Name of compacting material (as defined in ROCKS) In the following, M is the material index.	
3	1-10	$p_{thr,ini}$	G10.4	Pa	Initial pressure threshold	$ptini(M)$
4	1-5		I5		Softening model	$ifsoft(M)$
	11-20		G10.4		Parameter 1 of softening model	$fsoft(M,1)$
					...	
	71-80		G10.4		Parameter 7 of softening model	$fsoft(M,7)$
5	1-5		I5		Porosity model	$ifpor(M)$
	11-20		G10.4		Parameter 1 of porosity model	$fpor(M,1)$
					...	
	71-80		G10.4		Parameter 7 of porosity model	$fpor(M,7)$
6	1-5		I5		Permeability model	$ifper(M)$
	11-20		G10.4		Parameter 1 of permeability model	$fper(M,1)$
					...	
	71-80		G10.4		Parameter 7 of permeability model	$fper(M,7)$
7	31-40		G10.4	[1]	Permeability factor for ISO=1	$fiss_tensor(M,1)$
	31-40		G10.4	[1]	Permeability factor for ISO=2	$fiss_tensor(M,2)$
	31-40		G10.4	[1]	Permeability factor for ISO=3	$fiss_tensor(M,3)$
<i>Repeat line 2 to 7 for all dilating materials</i>						

11 GCOMP: Primary non-condensable gas component

Air is the primary non-condensable gas component of EOS7 and EOS7R, which usually is an appropriate choice for the time immediately after repository closure. Due to gas-producing processes, other gas components may evolve and become predominant. Module GCOMP allows to change characteristics of the primary non-condensable gas component in terms of absolute molecular weight M_{gas} , specific enthalpy h_{gas} , inverse Henry constant H_{inv} , and viscosity of the gas-vapour mixture.

11.1 Absolute molecular weight

The absolute molecular weight of the non-condensable gas can be changed by input parameter M_{ncg} (`GCOMP_AM`), which has to be defined in units of kg/mol (note that the absolute molecular weight variables `AMA` of EOS7 and EOS7R are defined in units of g/mol). Because the composition of the main gas component can change with time and place, M_{ncg} might not be the correct molecular weight for the entire simulation. However, many processes are not sensitive to errors in molecular weight if the amount of substance is correct. This applies to

- partial pressures (because EOS7 and EOS7R assume ideal gasses),
- the Henry law (which only depends on the amount of substance),
- advective flow of the gas component (because the mass of dissolved gas usually is too small to influence fluid density), and
- diffusive flow of the gas component in the liquid phase (which only depends on the amount of substance).

Simulations may therefore use erroneous molecular weights of the primary non-condensable gas component. These errors affect component masses but not their amount of substance.

11.2 Specific enthalpy

By setting $h_{\text{gas}} > 0$ (`GCOMP_CV`), the specific enthalpy of the main non-condensable gas component is set to h_{gas} . In case of $h_{\text{gas}} \leq 0$, the default value of the respective EOS

module is used, which is 733 J/mol for EOS7 and EOS7R (air), and 10,170 J/mol for EOS5 (hydrogen).

11.3 Inverse Henry constant

The temperature-dependency of the inverse Henry is calculated using a cubic polynomial with lower cut-off $H_{inv,min}$

$$H_{inv} = \max(H_{inv,min}, a_1 + a_2\vartheta + a_3\vartheta^2), \quad (11.1)$$

where ϑ is the temperature in degree Celsius. The equation is only applied if $H_{inv} \neq 0$. Otherwise, GCOMP uses the inverse Henry constant of the EOS module.

11.4 Gas phase viscosity

The GCOMP module offers three viscosity functions for vapour-bearing gases:

- **Hydrogen only (no vapour)**

`GCOMP_VISFUN = "H2"` selects the viscosity function of the EOS5 module.

- **Air and vapour**

`GCOMP_VISFUN = "Air-H2O"` selects the viscosity function of the EOS7 and EOS7R module.

- **Hydrogen and vapour**

This viscosity function is selected by `GCOMP_VISFUN = "H2-H2O"`.

Viscosity function 3 is based on the temperature-dependent viscosity function of /LAN 69/ for a H₂-vapour mixture, which we have extended by a pressure-dependent correction factor $h(p)$:

$$\eta_{H_2}(T, p, x_{H_2}) = f(T) \cdot g(x_{H_2}) \cdot h(p) \cdot 191.8 \cdot 10^{-7} \text{ Pa s}. \quad (11.2)$$

T is the temperature in Kelvin, p is the gas pressure, and x_{H_2} the mass fraction of H₂. The function $f(T)$ is given by

$$f(T) = \left(\frac{T}{273.16 \text{ K}} \right)^n \quad (11.3)$$

with

$$n = x_{\text{H}_2} \left(0.674 - 0.034 \cdot 10^{-4} \frac{\vartheta}{1^\circ\text{C}} \right) + x_{\text{H}_2\text{O}} \left(1.082 - 0.25 \cdot 10^{-4} \frac{\vartheta}{1^\circ\text{C}} \right). \quad (11.4)$$

Function $g(x_{\text{H}_2})$ is defined by

$$g(x_{\text{H}_2}, x_{\text{H}_2\text{O}}) = \left(1 + \sqrt{2 (2.016 x_{\text{H}_2} + 18.016 x_{\text{H}_2\text{O}})} \right) \frac{0.6355 x_{\text{H}_2} + 0.439 x_{\text{H}_2\text{O}}}{4.36 x_{\text{H}_2} + 6.31 x_{\text{H}_2\text{O}}} \quad (11.5)$$

with $x_{\text{H}_2\text{O}} = 1 - x_{\text{H}_2}$.

The pressure-dependency of the viscosity

$$h(p) = \left(\frac{p}{101325 \text{ Pa}} \right)^{0.005} \quad (11.6)$$

has been derived from the relation that is implemented in the viscosity routine of EOS5 for pure hydrogen. It has to be regarded as an approximation.

11.5 Input data

The input parameters of module GCOMP are summarized in Tab. 11.1.

Tab. 11.1 Input format of data block GCOMP

Line	Column	Vontent	Format	Unit	Description	Variable
1	1-5	"GCOMP"	A5		Keyword	
2	1-10	M_{ncg}	G10.4	kg/mol	Absolute molecular weight	GCOMP_AM
2	11-20	h_{gas}	G10.4	J/mol	Specific enthalpy	GCOMP_CV
2	21-30	a_1	G10.4	Pa ⁻¹	Coefficient 1 for the calculation of the inverse Henry constant	GCOMP_HC1
2	31-40	a_2	G10.4	Pa ⁻¹ °C ⁻¹	Coefficient 2 for the calculation of the inverse Henry constant	GCOMP_HC2
2	41-50	a_3	G10.4	Pa ⁻¹ °C ⁻²	Coefficient 3 for the calculation of the inverse Henry constant	GCOMP_HC3
2	51-60	$H_{inv,min}$	G10.4	Pa ⁻¹	Minimum value for the inverse Henry constant	GCOMP_HCMIN
2	61-70	"Air-H2O", "H2-H2O" or "H2"	A10		Viscosity function selector	GCOMP_VISFUN

12 PRLIM: Gas pressure limitation

12.1 Model and implementation

Modelling grids for repositories in rock salt usually do not include the impermeable host rock. However, it may happen that the host rock becomes permeable to gas flow if gas pressures approach the minimal principal stress by the opening of fissures or fractures. The escape of gas from the repository into the host rock can be modelled even if the host rock is not part of the modelling grid. For this purpose, module PRLIM clips the gas pressures inside the model to the desired threshold pressure. The accumulated loss of gas due to the clipping is printed.

Microscopic pathway can already open below the minimal principal stress due to microscopic heterogeneities of the material and stress field. The entry pressure is therefore defined relative to the minimal principal stress by means of a pressure offset Δ_{dilat} :

$$p_{\text{entry}} = \sigma_{\text{min}} - \Delta_{\text{dilat}}. \quad (12.1)$$

Module PRLIM allows to define parameter Δ_{dilat} separately for every material. Module PRLIM introduces minimal principal stress σ_{min} as a linear function of depth z

$$\sigma_{\text{min}}(z) = \sigma_{\text{min,ref}} + (z - z_{\text{ref}}) \frac{d\sigma_{\text{min}}}{dz}. \quad (12.2)$$

Parameter $\sigma_{\text{min,ref}}$ is the minimal principal stress at reference depth z_{ref} and the factor $d\sigma_{\text{min}}/dz > 0$ is the vertical gradient of the minimal principal stress. We neglect that stresses can change in the vicinity of mining cavities.

12.2 Input data

Tab. 12.1 shows the input data block of module PRLIM.

Tab. 12.1 Input format of data block PRLIM

Line	Column	Content	Format	Unit	Description	Variable
1	1-5	"PRLIM"	A5		Keyword	
2	1-10	z_{ref}	G10.4	m		PRLIM_ZREF
2	11-20	$\sigma_{min,ref}$	G10.4	Pa		PRLIM_P
2	21-30	$\frac{d\sigma_{min}}{dz}$	G10.4	Pa/m		PRLIM_DPDZ
3	1-5	Material name	A5		Activate PRLIM for this material. M ist he material index in the following	
3	6-15	Δ_{dilat}	G10.4	Pa	Δ_{dilat}	PRLIM_POFFSET (M)
<i>Repeat line 3 for all materials that introduce pressure limitation</i>						

13 PTIME: High-precision printout times

Module PTIME works in the same way as data block TIMES except for the higher precision of time values and the extension to 10,000 time entries. If data block PTIME is present, it overwrites the TIMES block. Tab. 13.1 shows the structure of the PTIME data block, which resembles data block TIMES.

Tab. 13.1 Input format of data block PTIME

Line	Column	Content	Format	Unit	Description	Variable
1	1-5	"PTIME"	A5		Keyword	
2	1-5	Number of times in table	I5	1	Must not be larger than 100	ITI
2	6-10	Number of times to be used	I5	1	Must be larger or equal to ITI. If larger than ITI, printout times will be distributed according to TINTER.	ITE
2	11-20	Maximum time step	G10.4	s	Upper limit for the time step size after first printout time. Inactive if zero.	DELAF
2	21-30	Time increment for printouts ITI to ITE	G10.4	s	Only active if ITE > ITI	TINTER
≥3	1-20, 21-40, 41-60, 61-80	Table of printout times (ascending order)	4G20.14	s		TIS(I)

14 RANGE: Limiting primary variables

Transitions between one-phase states and two-phase states can be numerically problematic causing bad convergence and a drastic reduction of time step size. A possible workaround is to keep the system in a two-phase state by restricting gas saturation to values above 0 and below 1.

Another numerical problem is that brine mass fraction can run out of bounds if water saturation is very low. The reason is that erroneous brine mass fractions do not violate the absolute convergence criterion if liquid saturation is very small. Brine mass fractions beyond physical meaning need not be a numerical problem but they hinder a meaningful visualisation of the brine mass fraction. One might therefore want to clip the brine mass fraction to reasonable values.

The RANGE module allows to restrict the range of both, gas saturation and brine mass fraction. This can involve a clipping of primary variables that violates mass conservation. The physical system parameter should therefore be chosen such that clipping is avoided as far as possible.

14.1 Limiting brine mass fraction

Brines are defined by the equation-of-state modules EOS7 and EOS7R as mixture of pure water and a reference brine. The mass ratio between the reference brine and the liquid is the brine mass fraction. Following this concept, the brine mass fraction cannot be larger than 1 without sacrificing the idea of mixing two liquids. However, if the specified reference brine is regarded as an intermediate mixing product, brine mass fractions beyond 1 can be physically plausible and TOUGH2 does not object to such values.

Errors in the estimation of the brine mass fraction do not necessarily lead to a violation of convergence criteria because the convergence criteria evaluate mass conservation, not mass fraction conservation. If liquid saturation is low, the absolute errors of brine mass are small too. TOUGH2 therefore tolerates large errors in brine mass fraction if grid elements are almost dry. In turn, the estimated brine mass fraction may exceed the value of 1 by far. This is not a problem in terms of mass conservation but may contra-

dict the idea of mixing two types of liquid. Grid elements with very high brine mass fractions also complicate the visual interpretation of the simulation output.

By setting `RANGE_restrictXb = 1`, the brine mass fraction is restricted to the interval `[RANGE_XBmin, RANGE_XBmax]`. This is achieved by clipping the values of the corresponding primary variable. For the reasons mentioned above, this should not significantly violate mass conservation. Setting `RANGE_XBmin = 0` and `RANGE_XBmax = 1` should be appropriate in many cases unless other process modules like CORFL require brine mass fractions above 1.

14.2 Constant brine mass fraction

Setting `RANGE_equilibrateXb = 1` keeps the brine mass fraction at a constant value `RANGE_EQ_Xbr`. The intention may be to simulate a chemical equilibrium of the solution with salt rock, which would result in a constant brine mass fraction.

If the RANGE module keeps the brine mass fraction constant it conserves the total water mass. This includes the water implicitly contained in the reference brine. The ratio between brine mass and contained water mass is passed by parameter `RANGE_EQ_BrineMassPerWaterMass`.

Keeping the brine mass fraction constant is incompatible with the CORFL module, because this module uses the brine mass fraction as a marker for the fluid's corrosion capability. The interference with the CORRO module is not well tested.

14.3 Clipping gas saturation and reducing vapour pressure

Setting `RANGE_restrictSg = 1` restricts *gas saturation* (a primary variable) to the interval `RANGE_SGmin` to `RANGE_SGmax`. Choosing `RANGE_SGmin > 0` and `RANGE_SGmax < 1` preserves a two-phase state. The clipping operation involved violates mass conservation and should therefore be avoided as much as possible. The system should be designed to remain in a two-phase state by itself, for example by introducing residual saturations to the relative permeability function. Further on, capillary pressures may prevent desaturation of elements. Yet, the disappearance of a phase cannot be entirely prevented by these measures for the following reasons:

- Even an immobile gas phase can be displaced by way of gas dissolution and advective transport of dissolved gas in the liquid phase.
- Even an immobile liquid phase can be displaced by evaporation and advective transport of vapour in the gas phase.
- Backfill compaction, induced by the COMP module, compresses the gas phase thereby increasing gas dissolution. If the liquid saturation is near to one the gas phase can disappear.

To prevent evaporation of the entire liquid phase, the RANGE module also offers to reduce the saturation vapour pressure. By setting `RANGE_reducePs = 1` the vapour pressure decreases linearly to zero as gas saturation increases from `RANGE_PS_Sgmin` to `RANGE_PS_Sgmax`. The user should set `RANGE_PS_Sgmax < RANGE_Sgmax` to prevent the RANGE module from clipping the gas saturation (see Fig. 14.1).

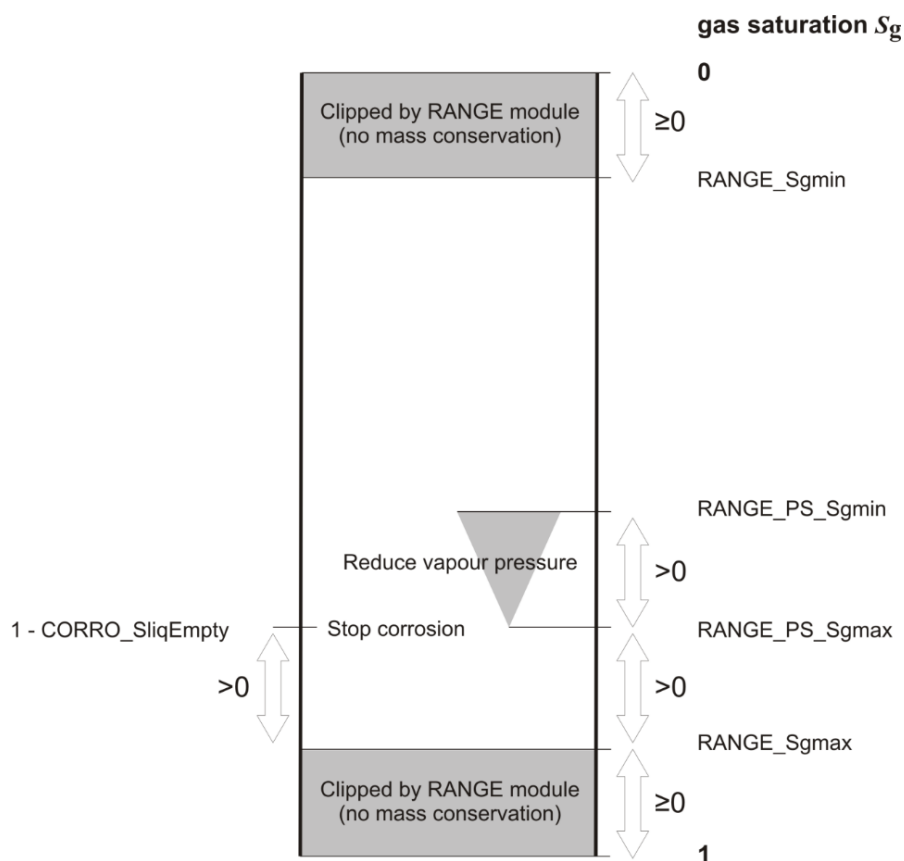


Fig. 14.1 Relationship between saturation limits of the RANGE and CORRO modules

14.4 Input data

The input parameters of module RANGE are listed in Tab. 14.1.

Tab. 14.1 Input format of data block RANGE

Line	Column	Content	Format	Unit	Variables
1	1-5	Keyword "RANGE"	A5		
2	1-10	Limit brine mass fraction? 0: No. 1: Yes. Restrict to interval $[X_{b,min}, X_{b,max}]$.	G10.4	1	RANGE_restrictXb
2	11-20	Lower limit of the brine mass fraction	G10.4	1	RANGE_XBmin
2	21-30	Upper limit of the brine mass fraction	G10.4	1	RANGE_XBmax
3	1-10	Constant brine mass fraction? 0: No 1: Yes.	G10.4	1	RANGE_equilibrateXb
3	11-20	Brine mass fraction in equilibrium.	G10.4	1	RANGE_EQ_Xbr
3	21-30	Brine mass per mass of contained water.	G10.4	1	RANGE_EQ_BrineMassPerWaterMass
4	1-10	Limit gas saturation? 0: No. 1: Yes.	G10.4	1	RANGE_restrictSg
4	11-20	Lower limit of gas saturation	G10.4	1	RANGE_SGmin
4	21-30	Upper limit of gas saturation (has to be larger than the lower limit)	G10.4	1	RANGE_SGmax
5	1-10	Dim saturation vapour pressure? 0: No. 1: Yes. Reduce saturation vapour pressure linearly as gas saturation rises from $S_{g,dim}$ to $S_{g,zero}$. $S_{g,dim} < S_{g,zero} \leq 1$	G10.4	1	RANGE_reducePs
5	11-20	$S_{g,dim}$	G10.4	1	RANGE_PS_SGmin
5	21-30	$S_{g,zero}$	G10.4	1	RANGE_PS_SGmax

15 RELA: permeability and capillary pressure functions

The RELA module introduces functional dependencies for permeability and capillary pressure. For reasons of downward compatibility, these functions are also part of the COMP module. However, the user is advised to use the corresponding features of the RELA module, which override those of the COMP module.

15.1 Porosity-permeability relationships

Experimental studies with compacting salt grit have shown power law relationships between permeability and porosity for certain porosity ranges /KRÖ 09/. The COMP module introduces piecewise-defined porosity-permeability relationships with up to five power subfunctions

$$k = a_i \phi^{b_i} \quad (15.1)$$

with k being the (isotropic) intrinsic permeability and ϕ the porosity. Parameters a_i and b_i ($1 \leq i \leq 5$) are fitting parameters.

The porosity domain of each subfunction is determined by the intersections of adjacent subfunctions i and $i + 1$. Subfunctions must be defined in the order of descending porosity in input data block COMP meaning that subfunction i refers to higher porosities than subfunction $j > i$.

Permeability is set to zero if the lower porosity limit $\phi_{k=0}$ is set to a positive value

$$k = 0 \quad \text{for } \phi \leq \phi_{k=0} . \quad (15.2)$$

Note that only isotropic permeabilities are available.

15.2 Change of capillary pressures

Backfill compaction affects capillary pressures by changing the backfill's pore structure. The COMP module allows to approximate this effect by means of the Leverett's J-function /LEV 41/

$$p_c(S) = p_{c0}(S) \left(\frac{k_0 \phi}{\phi_0 k} \right)^\alpha. \quad (15.3)$$

p_c is the capillary pressure at liquid saturation S , porosity ϕ , and permeability k . Function $p_{c0}(S)$ is the unscaled capillary pressure function of the initial porosity ϕ_0 and permeability k_0 as defined by data block ROCKS. If the user chooses p_{c0} to be the van Genuchten function (ICP = 7), the maximum capillary pressure cut-off $CP(4)$ is applied to the scaled function, too.

15.3 Temperature-dependent capillary pressures

According to /GRA 14/, capillary pressure decreases with temperature, and capillary pressure functions for different temperatures relate to each other by

$$p_c(S, T) = p_c(S, T_{\text{ref}}) \frac{\beta + (T + 273.15)}{\beta + (T_{\text{ref}} + 273.15)}, \quad (15.4)$$

where T is the temperature in °C and $p_c(S, T_{\text{ref}})$ the capillary pressure function at temperature T_{ref} (also in °C). Constant β is defined by

$$\beta := \frac{a}{b} \quad (15.5)$$

with a and b being constants of the dependency of the liquid-gas interface tension on temperature

$$\gamma^{\text{lg}} = a + b (T + 273.15) \quad (15.6)$$

According to /GRA 14/, β varies between -800 K and -330 K and values of -566 K and 438 K have been found for silt loam. Both input parameters of the RELA data block, β and T_{ref} , are input in degrees Celsius.

15.4 Input data

The input data of module RELA are listed in Tab. 15.1.

Tab. 15.1 Input format of data block RELA

Line	Column	Content	Format	Unit	Description	Variable
1	1-5	"RELA"	A5		Keyword	
2	1-5	Material name	A5		Name of compacting material (see card ROCKS). M is the material index.	
3	1-10	K_{ref}	G10.4	[sec ⁻¹]	Reference convergence rate	COMP_KREF (M)
	11-20	f_{loc}	G10.4	[1]	Local modification of the reference convergence rate	COMP_FLOC (M)
	21-30	p_G	G10.4	[Pa]	Lithostatic pressure at the location if no cavity would exist	COMP_PG (M)
	31-40	m_p $= m_\phi$	G10.4	[1]	Exponent for the calculation of f_p	COMP_M (M)
	41-50	ϕ_r	G10.4	[1]	Porosity at which backfill support commences	COMP_PHIref (M)
	51-60	h_1	G10.4	[1]	Parameter for the calculation of f_ϕ	COMP_H1 (M)
	61-70	g_1	G10.4	[1]	Parameter for the calculation of f_ϕ	COMP_G1 (M)
	71-80	g_2	G10.4	[1]	Parameter for the calculation of f_ϕ	COMP_G2 (M)
4	1-10	λ_s	G10.4	[1]	Parameter for the calculation of f_T	COMP_LAMBDA (M)
	11-20	K_0	G10.4	[sec ⁻¹]	Initial convergence rate	COMP_K0 (M)
	21-30	a	G10.4	[1]	Weighting factor for creep processes	COMP_A (M)
	31-40	Q_1	G10.4	[J/mol]	Activation energy for creep process 1	COMP_Q1 (M)
	41-50	Q_2	G10.4	[J/mol]	Activation energy for creep process 2	COMP_Q2 (M)
	51-60	T_{ref}	G10.4	[°C]	Temperature of the rock at the reference location	COMP_TGREF (M)
	61-70	ϕ_{lim}	G10.4	[1]	Lower porosity limit for the convergence process (may be 0)	COMP_PHIMIN (M)
5	1-10	0 or 1	I10	[1]	Enable Leverett scaling of capillary pressures? (0 = no, 1 = yes)	COMP_LEVQ (M)
	11-20	k_0	G10.4	[m ²]	Reference permeability for Leverett scaling	COMP_LEVPERREF (M)
	21-30	ϕ_0	G10.4	[1]	Reference porosity for Leverett scaling	COMP_LEVPHIREF (M)
	31-40	α	G10.4	[1]	Exponent of the Leverett scaling	COMP_LEVEXP (M)
6	1-10	$\phi_{k=0}$	G10.4	[1]	Permeability will be 0 for porosities $\leq \phi_{k=0}$	COMP_CUTOFF (M)
7	1-10	n_{sec}	I10	[1]	Number of subsections of the porosity-permeability relation	COMP_NBRANCH (M)
8	1-10	a_i	G10.4	[m ²]	Factor of power law i	COMP_PERA (I, M)
	11-20	b_i	G10.4	[m ²]	Exponent of power law i	COMP_PERB (I, M)
<i>Repeat line 8 for all n_{sec} sections</i>						
last	1-10	0 or 1	I10	1	Enable temperature-dependent capillary pressures? (0 = no, 1 = yes)	COMP_LEVQ (M)
	11-20	β	G10.4	°C		rela_PCTBETA (M)
	21-30	T_{ref}	G10.4	°C		rela_PCTTREF (M)
<i>Repeat from line 2 for all materials concerned</i>						

16 RN

Module RN simulates decay, transport, sorption and anion exclusion of radionuclide chains of arbitrary size. It operates on top of the TOUGH2 flow simulation without affecting them. The module can therefore be used with every EOS module.

16.1 Links to standard TOUGH2

The RN module calculates the decay of radionuclides first. In every time step of the ensuing transport calculation, the phase distribution of radionuclides is determined as well as the advective and diffusive radionuclide fluxes.

The transport equations were taken from the TOUGH2 core to achieve the same transport behavior. The equations describing the phase distribution of radionuclides are derived from the equations of the EOS7R module but also include linear sorption.

Required transport parameters like, for instance, weighting parameters, are obtained from the regular TOUGH2 input. However, there is a little difference regarding the NB parameter of block MULTI because diffusive transport of radionuclides is also possible if no diffusion ($NB=6$) is selected in MULTI.

Please note that the radionuclide masses placed in the system with the RN module are *total* masses. They are composed of the masses in all phases (solid, liquid, and gas). On the contrary, radionuclide masses placed in a two-phase state in connection with the EOS7R module are dissolved masses *after the distribution process* and do not include adsorbed masses or masses in the gas phase.

16.2 Time stepping and performance

The RN module uses a time integration algorithm that implements the Bulirsch-Stoer method /STO 80/. Owing to this new solver there are now three steps of time discretization:

1. Time discretization by the CYCIT routine of TOUGH2 yielding time step size Δt_{T2} (which is the standard time step size $DELTEX$ of TOUGH2).

2. The subdivision of Δt_{t2} by the time stepping routine of the Bulirsch-Stoer solver yielding the time step size Δt_{BS} .
3. The successive subdivision of Δt_{BS} in 2, 4, 6, 8, 10, 12, 14, 16, and 18 equal parts used for the extrapolation part of the Bulirsch-Stoer method. The successive division of Δt_{BS} is stopped as soon as convergence is achieved. We use n_{ex} to refer to the number of subdivisions made.

Convergence is tested in step 3. If convergence is not achieved, three things can happen:

- Time step Δt_{BS} is further subdivided (n_{ex} is increased)
- Time step Δt_{BS} is reduced
- Time step Δt_{T2} is reduced

For some problems, the performance of the simulation heavily depends on how these measures are balanced. To achieve good performance, the numerical effort that has been made before a time step is discarded should be as low as possible. Particularly, it has to be decided whether a reduction of Δt_{BS} is a better choice than an increase of n_{ex} . Although increasing n_{ex} improves the quality of extrapolation it is connected with a non-linear increase of calculation time, partly due to the mounting inter-process communication of TOUGH2-MP-GRS. Reduction of Δt_{BS} appears to be a better choice if convergence by subdivision of Δt_{BS} is not achieved quickly. We therefore stop increasing n_{ex} and reduce Δt_{BS} instead, if the errors for each n_{ex} do not decrease by a factor of f_{ex} . For some problems, $f_{ex} = 0.6$ has yielded a speed increase by a factor of about 10.

Radionuclides that are very mobile should be defined first in data block RN. The reason is that TOUGH2-GRS and TOUGH2-MP-GRS handle radionuclides in the succession of their definition and that mobile radionuclides are the ones that most likely introduce convergence problems. Defining them first spares transport calculations for the less problematic radionuclides.

The RN module is the only process module that simulates fluxes between elements. For this reason, its overhead due to inter-process communication is considerably higher than for other process modules (so called “external elements” have to be exchanged). If many radionuclides are present the serial code TOUGH2-GRS can show a better performance than the multi-processor code TOUGH2-MP-GRS.

16.3 Simulation controls

Parameters controlling accuracy and performance are conveyed by the first line of data block RN. These are, in order of definition:

- Relative tolerance (default: 1E-7)
- Absolute tolerance in kg (default: 1E-30 kg)
- Maximum steps of the Burlirsch-Stoer stepper (default: 1000)
- Choice of the extrapolation routine (0: polynomial, 1: rational)
- Reduction factor for the TOUGH2 time step Δt_{T2} if the BS stepper has reached the maximum number of time steps (default: 0.2)
- Error reduction factor f_{ex} with $0 < f_{ex} < 1$ (default: 0.6)

The absolute tolerance decides on convergence if radionuclide quantities are small. If the absolute tolerance criterion is met for a specific radionuclide and location, transport and decay calculations are skipped.

Please note that adequate convergence criteria depend on the problem to be solved. Both, tolerance criteria and simulation controls of the RN module are likely to be further developed in the future.

16.4 Decay and adsorption of Nuclides

Radioactive decay is calculated for each time step Δt_{T2} using an exponential decay law for each radionuclide:

$$N(t + \Delta t_{T2}) = N(t)e^{-\lambda\Delta t_{T2}} \quad (16.1)$$

N is the amount of the radionuclide (mol), λ the radioactive decay constant with

$$\lambda = \frac{\ln 2}{T_{1/2}}, \quad (16.2)$$

and $T_{1/2}$ the half-life of the radionuclide. The exponential decay function improves the implementation of TOUGH2, which uses a linear decay function with lower accuracy.

Since the radioactive decay is calculated for the entire time step, Δt_{T2} should be kept smaller than the half-life of radionuclides in order to achieve sufficient accuracy. This may impose a performance problem which should be subject to future code development.

16.5 Anion exclusion

Usually, the pore space of argillaceous rocks is not fully accessible to anions, which are forced to the pore centres by the negative charge of mineral surfaces. This process is called anion exclusion and it can affect both, the advective and diffusive transport of radionuclides. In order to keep our model simple we assume that there is a sharp transition between the pore space accessible to anions and to that which is not. We will formulate our model for a single phase and a single anion to keep the description simple.

Advective transport of anions

TOUGH2 calculates the advective mass flow F_{adv} of a component (in kg/sec) by multiplying the mass flow of the fluid F_{phase} by the mass fraction X of the transported component:

$$F_{adv} = F_{phase} X \quad (16.3)$$

We use a similar approach for the advective transport of an anion in restricted pore space

$$F_{adv} = \hat{F}_{phase} \hat{X}. \quad (16.4)$$

\hat{F}_{phase} denotes the flow of fluid in restricted pore space and \hat{X} the anion's mass fraction in the fluid. If ϕ is porosity and ϕ_{ex} the porosity from which anions are excluded, \hat{X} and X are related by

$$\hat{X} = X \frac{\phi}{1 - \phi_{ex}} \quad (16.5)$$

because of the different fluid masses they refer to.

Obviously \hat{X} is larger than X but on the other hand, \hat{F}_{phase} must be smaller than or equal to the total fluid flow F_{phase} .

To understand how \hat{X} and \hat{F}_{phase} interact we consider the physically impossible case that particle velocities are the same at every point of the pore space. Under these unrealistic conditions the restriction of anions to pore centers would have no influence on anion flow. Obviously, anion exclusion enhances advective anion transport only if the flow densities in the accessible pore space are higher than in the inaccessible pore space (which can be expected in reality). The effect of anion exclusion therefore depends on the heterogeneity of the flow field, which has to be expressed by a relation between \hat{F}_{phase} and F_{phase} . We use

$$\hat{F}_{\text{phase}} = F_{\text{phase}} (1 - R_{\text{flow}}) \quad (16.6)$$

for this purpose, where R_{flow} is the fraction of the flow that is inaccessible to anions. The highest anion flow is achieved by $R_{\text{flow}} = 0$ meaning that the entire flow takes place in the accessible pore space. In the discrete version of this equation the element-specific variable R_{flow} is weighted using the WUP parameter of input block PARAM.

In order to obtain R_{flow} , we revisit the above example of constant particle velocities. We have reasoned that anion exclusion should have no effect with constant particle velocities. This means that

$$\hat{F}_{\text{phase}} \hat{X} = F_{\text{phase}} X. \quad (16.7)$$

From this we can conclude that

$$R_{\text{flow}} = 1 - \frac{X}{\hat{X}} = \frac{1 - \phi_{\text{ex}}}{\phi}. \quad (16.8)$$

Consequently, the condition

$$0 \leq R_{\text{flow}} < \frac{1 - \phi_{\text{ex}}}{\phi} \quad (16.9)$$

should be met for natural porous media.

The case $R_{\text{flow}} = 0$ is particularly interesting for the derivation of benchmark calculations. Let us consider two systems, one without anion exclusion and porosity ϕ_1 and another with anion exclusion and porosity ϕ_2 . If we set R_{flow} to zero, the entire flow takes place in the anion-accessible pore space. Under these circumstances, anion transport should be the same in both systems if the anion-accessible porosity of the second system $\phi_2 - \phi_{\text{ex}}$ is equal to ϕ_1 . This also applies to the diffusive transport described below.

Diffusive transport of anions

TOUGH2's flow equation for the diffusive transport of a component between two grid elements is

$$F_{\text{diff}} = -A \phi \tau \rho d \nabla X \quad (16.10)$$

where d is the molecular diffusion coefficient, ρ the density of the phase, τ a geometry factor that can be determined in several ways, ϕ porosity, and A the interface area between the two grid elements. Factor $A\phi$ is the interface area for the transport. The geometry factor τ captures effects of contorted flow paths and unsaturated conditions. Note that τ decreases with increasing tortuosity of flow paths.

For anion exclusion, ϕ , τ and X have to be substituted by corresponding parameters for the restricted flow path:

$$F_{\text{diff}} = -A \hat{\phi} \hat{\tau} \rho d \nabla \hat{X} \quad (16.11)$$

\hat{X} has already been introduced and the new flow cross section $\hat{\phi}$ can be set equal to $\phi - \phi_{\text{ex}}$. We set the geometry factor to

$$\hat{\tau} = \tau(1 - R_{\text{tort}}) \quad (16.12)$$

using a reducing factor $1 - R_{\text{tort}}$, which should be smaller than one. Variables ϕ and τ are element specific. For element connections they are calculated in the same way as d using a weighted harmonic mean.

In homogeneous material and if the geometry factor remains unchanged ($R_{\text{tort}} = 0$) the diffusive flow remains unchanged too, because $\hat{\phi} \nabla \hat{X} = \phi \nabla X$. Yet, under transient con-

ditions, anion exclusion still has an effect on diffusive transport owing to the fact that pore space is restricted and less flow is needed to propagate a diffusive front.

A note on inactive and active elements

Radionuclides are introduced to active elements by prescribing radionuclide masses. From a physical point of view, these masses are only present in the pore space that is accessible to anions. Mean concentrations are obtained by dividing anion masses by the total pore volume. To obtain concentrations inside the accessible pore volume, radionuclide masses must be divided by the accessible pore volume.

Inactive elements require the prescription of mass concentrations in the accessible pore volume because of their unknown volume. Concentrations refer to radionuclide masses per *accessible* pore volume.

16.6 Extended mobilization models

The extended models for radionuclide mobilisation are not yet fully implemented and tested. Nevertheless, we will already describe the concept here.

16.6.1 New commands

The standard method of placing radionuclides in the system is by using the command “`place`” (see chapter 16.7). This command places the mass of a certain radionuclide in a material. The command specifies a mobilization time. Until that time, radionuclides remain immobile and are subject to radioactive decay. Additional mobilization models are introduced by the commands “`container`”, “`bond`” and “`rn`”. These commands are motivated as follows.

We assume that radionuclides are contained in a waste container by different bonds. For instance, the instant release fraction represents a certain bond type, but radionuclides can also be bound to a corroding waste matrix. Models for the mobilization of radionuclides from a specific bond will be called “bond models” in the following.

The release of radionuclides depends on the time of canisters failure too. We introduce “canister failure models” to describe the failure of a certain canister type. Canister fail-

ure models are not assigned to a single container but to a group of containers of same type.

Eventually, a “mobilization model” is a combination of a bond model and a canister failure model. Mobilization models take the general form

$$\dot{Q}(i, t) = n(t)\dot{Q}_{\text{pmob}}(i, t), \quad (16.13)$$

$\dot{Q}(i, t)$: mobilization rate, i. e. mobilized mass per time for radionuclide i at time t in kg/s
 $n(t) = N_{\text{fail}}(t)/N_{\text{tot}}$: fraction of canisters that have failed
 \dot{Q}_{pmob} : rate of mobilization from the bond in kg/s

with $\dot{n}(t)$ being the canister failure model and $\dot{Q}_{\text{pmob}}(i, t)$ the bond model. The following commands are introduced for the definition of mobilization models (see also Tab. 16.2):

- The “`container`” command defines the location of a canister group and a corresponding container failure model.
- The “`bond`” command adds a bond type to the canister group that has been defined last (that is the last “`canister`” command).
- The “`rn`” command assigns radionuclides of a certain mass to the bond and canister group that have been defined last.

Radionuclides introduced in this way are not visible in the simulation output before they are mobilized.

16.6.2 Canister failure models

Canister failure models refer to a group of canisters (preferably of same type). The discrete failure of canisters is approximated by a continuous function, which is the canister failure model.

Canister failure models define a “trigger event” that starts the failure process. No canister fails before that event. The trigger event can be the start of the simulation (then there actually is no trigger) but also the accomplishment of a certain liquid saturation.

For the time being there are two canister failure models: a constant failure rate and a normal distribution of failures.

Constant failure rate

A constant failure rate stands for a uniform distribution of canister life times. The canister failure rate is

$$\dot{n}(t) = \frac{\dot{N}_{\text{fail}}(t)}{N_{\text{tot}}} = \begin{cases} 0 & \text{for } t < t_{\text{tw}} \\ 1/t_{\text{conf}} & \text{for } t_{\text{tw}} \leq t < t_{\text{tw}} + t_{\text{conf}} \\ 0 & \text{for } t > t_{\text{tw}} + t_{\text{conf}} \end{cases} \quad (16.14)$$

$N_{\text{fail}}(t), \dot{N}_{\text{fail}}(t)$: number of canisters that have failed, and failure rate

N_{tot} : number of canisters

$t_{\text{tw}} := t_{\text{trig}} + t_{\text{wait}}$ with

$t_{\text{trig}} \geq 0$: time of the trigger event

$t_{\text{wait}} \geq 0$: time between trigger event and first failure

$t_{\text{conf}} \geq 0$: here: time between first and last canister failure

The fraction of canisters that have failed is

$$n(t) = \frac{N_{\text{fail}}(t)}{N_{\text{tot}}} = \begin{cases} 0 & \text{for } t < t_{\text{tw}} \\ \frac{t - t_{\text{tw}}}{t_{\text{conf}}} & \text{for } t_{\text{tw}} \leq t < (t_{\text{tw}} + t_{\text{conf}}) \\ 1 & \text{for } t > (t_{\text{tw}} + t_{\text{conf}}) \end{cases} \quad (16.15)$$

The "canister" command requires the following numerical input parameters:

1. Selector for container failure model. Set to 1 for a constant rate.
2. Selector for the trigger event: Set to 0 for no trigger and to 1 for the excess of a certain liquid saturation.
3. Critical liquid saturation (for trigger event 1).
4. t_{conf} . Meaning here the time between the first and the last failure event. Set $t_{\text{conf}} = 0$ for instant failure of all canisters.
5. Waiting time t_{wait} between trigger event and the first failure.

Normal distribution of failures

This model assumes that all canisters have a similar resistance against corrosion but canister failure frequency varies around a mean confinement time t_{conf} according to a normal distribution. The canister failure rate is

$$\dot{n}(t) = \begin{cases} 0 & \text{for } t < t_{\text{trig}} \\ \frac{1}{\sqrt{2\pi}\sigma} e^{-\frac{1}{2}\left(\frac{(t-t_{\text{trig}})-t_{\text{conf}}}{\sigma}\right)^2} & \text{for } t \geq t_{\text{trig}} \end{cases} \quad (16.16)$$

$t_{\text{trig}} \geq 0$: time of the trigger event

$t_{\text{conf}} \geq 0$: here: mean canister life time

σ : standard deviation of the canister life time

The fraction of canisters that have failed is

$$n(t) = \frac{1}{2} \left(1 + \operatorname{erf} \left(\frac{(t - t_{\text{trig}}) - t_{\text{conf}}}{\sqrt{2\pi}\sigma} \right) \right) \quad (16.17)$$

The "canister" command requires the following numerical input parameters:

1. Selector for container failure model. Set to 2 for normal distribution.
2. Selector for the trigger event: Set to 0 for no trigger and to 1 for the excess of a certain liquid saturation.
3. Critical liquid saturation (for trigger event 1).
4. t_{conf} . Meaning here: mean canister life time
5. Standard deviation σ of the canister life time

16.6.3 Bond models

Bond models take the following general form:

$$\dot{Q}_{\text{pmob}}(i, t; T, \dots; T_{\text{acti}}, \dots) = \frac{m_{\text{ibin}}(i, t)}{m_{\text{bin}}(t)} \cdot (A_{\text{eff}} \cdot j_{\text{mobTr}}) \cdot e^{-T_{\text{acti}} \left(\frac{1}{T} - \frac{1}{T_{\text{ref}}} \right)} \quad (16.18)$$

$\dot{Q}_{\text{pmob}}(i, t, \dots)$: rate of mobilization from the bond in kg/s for radionuclide i at time t . This function may depend on state variables like, for example, temperature or liquid saturation.

T_{ref} : reference temperature in K.

T_{acti} : activation temperature in K. Set to 0 for no temperature dependency.

$m_{\text{ibin}}/m_{\text{bin}}$: mass fraction of radionuclide i in the bond.

A_{eff} : effective surface of waste canisters in m^2 .

j_{mobTr} : mobilization flow density j_{mobTr} at reference temperature T_{ref} in $\text{kg m}^{-2} \text{s}^{-1}$

The “bond” command requires the following numerical input parameters:

1. Selector for the bond model. Set to 1.
2. Selector for the type of function A_{eff} . Set to 0 for a constant function.
3. First parameter of function A_{eff} . Value of A_{eff} if a constant function has been selected.
4. Second parameter of function A_{eff} .
5. Third parameter of function A_{eff} .
6. Selector for type of function j_{mobTr} . Set to 0 for a constant function.
7. First parameter of function j_{mobTr} . Value of j_{mobTr} if a constant function has been selected.
8. Second parameter of function j_{mobTr} .
9. Third parameter of function j_{mobTr} .
10. Activation temperature T_{acti} . Set to 0 for no temperature dependency.
11. Reference temperature T_{ref} .

16.6.4 Implementation

The Bulirsch-Stoer solver of the RN module used for time integration requires processes that change radionuclide masses continuously. Discontinuous mobilization process-

es like, for example, instant release therefore cannot be part of the time integration algorithm. Discontinuous transfer of radionuclides from their bonds into the flow system has to be carried out *before* the Bulirsch-Stoer algorithm. In principle, continuous mobilization processes can be implemented in the same way. To keep the implementation simple, we use this kind of radionuclide transfer for discontinuous as well as for continuous mobilization models. However, there are two disadvantages connected to this procedure:

- The release time of a discontinuous release must not match the simulation time steps. This causes an error in release times. In principle, this can be solved by adapting the automatic time stepping control to the release times.
- Continuous releases do not benefit from the higher time discretization of the Bulirsch-Stoer solver.

16.7 Input data

Tab. 16.1 show the syntax of control parameters and radionuclide definitions. The following command section of the input is described in Tab. 16.2.

Tab. 16.1 Input format of data block RN

Line	Co-lumn	Content	For-mat	Unit	Description	Variable
1	1-10	Relative tolerance	G10.4	1	default: 1E-7	rncntrl_relTol
	11-20	Absolute tolerance	G10.4	kg	default: 1E-30 kg	rncntrl_absMtol
	21-30	Maximum steps of the Burlirsch-Stoer stepper	I10	1	default: 1000	rncntrl_maxstsp
	31-40	extrapolation routine	I10	1	0: polynomial (default), 1: rational	rncntrl_extrRout
	41-50	Reduction factor for the TOUGH2 time step Δt_{T2} if the BS stepper has reached the maximum number of time steps	G10.4	1	default: 0.2	rncntrl_dtFac
	51-60	Error reduction factor f_{ex} with $0 < f_{ex} < 1$	G10.4	1	default: 0.6	rncntrl_errFac
<i>Repeat the following lines for each radionuclide (RN) i</i>						
2+(i-1)	1-10	Radionuclide name	A10		Name of radionuclide (RN)	rn_NAME
	11-21	$T_{1/2}$	G10.4	s	Half-life of RN	rn_HALF
	21-30	RN Daughter name	A10		Name of daughter	rn_daughtername

Line	Co-lumn	Content	For-mat	Unit	Description	Variable
					RN	
	31-40	Molecular weight	G10.4	kg/mol	Molecular weight of RN	rn_M
	41-50	Henry constant or inverse Henry constant	G10.4	Pa or 1/Pa	Absolute value will be used. <0: use Henry constant >0: use inverse Henry constant	rn_H
	51-60	Solubility limit	G10.4	kg/m ³	Solubility limit	rn_Ceq
	61-70	Diffusivity in gas	G10.4	m ² /s	Diffusion constant in gas phase	rn_Dg
	71-80	Diffusivity in liquid	G10.4	m ² /s	Diffusion constant in liquid phase	rn_Dl
<i>This section closes with a "--" line, which signals, that a command section follows (see next table)</i>						

Tab. 16.2 Commands of module RN

See chapters 16.6.2 and 16.6.3 for the parameters of canister failure and bond models.

column 1 to 10	column 11 to 20	column 21 to 25	column 26+(i-1)*10 to 40+(i-1)*10
<i>command string (case insensitive)</i>	<i>string (A10)</i>	<i>string (A5)</i>	<i>list of numbers (G15.4)</i>
"place"	name of radionuclide (leave blank to select all radionuclides)	material name (leave blank to select all materials)	<i>active elements:</i> 1 st : initial radionuclide mass in kg. <i>inactive elements:</i> 1 st : initial radionuclide concentration in kg/m ³ . 2 nd : time of release in sec.
"retard"	name of radionuclide (leave blank to select all radionuclides)	material name (leave blank to select all materials)	1 st : K _d in m ³ /kg.
"exclusion"	name of radionuclide (leave blank to select all radionuclides)	material name (leave blank to select all materials)	1 st : excluded porosity fraction 2 nd : flow reduction (between 0 and 1) 3 rd : tortuosity reduction (between 0 and 1)
"container"	element name or material name	type of location ("E" for element, "M" for material)	1 st : container failure model (selector) next: parameters of container failure model
"bond"	<i>empty</i>	<i>empty</i>	1 st : selector for bond model (selector) next: parameters of bond model
"rn"	radionuclide name	<i>empty</i>	1 st : inserted mass in kg

17 Output

TOUGH2-GRS and TOUGH2-MP-GRS generate two types of printouts:

- Total system printouts to the files ELE_MAIN and CON_MAIN for prescribed times.
- Time series printouts to the files FOFT, COFT, GOFT, and DOFT for prescribed elements, connections, sources, and domains (rocks), respectively.

The total system printout to the output channel STDOUT still exists but is not maintained anymore and will therefore not be mentioned in the following.

The process modules of GRS have increased the number of output parameters. To reduce file sizes, the module CNTRL allows to skip printouts (see chapter 4.3.2). Time series files can also be generated in binary format. Whether the time series output uses text or binary format is controlled by the CNTRL module.

17.1 Global printouts for elements (ELE_MAIN)

Global printouts to file ELE_MAIN are generated at user-defined times (specified in data blocks TIMES or PTIME) as well as on the first and last time step. The printout holds element-specific output data formatted in the same way as the time series files:
time step number, time, [element index, [variables, ...], ...].

Tab. 17.1 Element-specific output parameters of TOUGH2-GRS

No TOUGH2- GRS	No TOUGH2- MP-GRS	Module (0 printed if inactive)	Parameter	Description	Unit
1	1		P_{gas}	gas pressure	Pa
2	2		$P_{\text{liq}} = P_{\text{gas}} + P_{\text{cap}}$	liquid pressure	Pa
3	3		S_{liq}	gas saturation	1
4	4		S_{gas}	liquid saturation	1
5	5		X_{brine}	brine concentration	1
6	6		T	temperature	°C
7	7		$-P_{\text{cap}}$	capillary pressure (P_{cap} is negative)	Pa
8	8		$P_{\text{pot}} := P_{\text{liq}} - zg\rho_{\text{liq}}$	pressure potential (only a potential if density is constant)	Pa
9	9		ρ_{gas}	density of the gas phase	kg/m ³
10	10		ρ_{liq}	density of the liquid phase	kg/m ³
11	11		μ_{gas}	viscosity of the gas phase	Pa s
12	12		μ_{liq}	viscosity of the liquid phase	Pa s
13	13		k	intrinsic permeability (ISO=1) multiplied by $V_{\text{phys}}/V_{\text{tough}}$	m ²
14	14		V_{tough}	initial element volume	m ³
15	15	COMP otherwise 1	$V_{\text{phys}}/V_{\text{tough}}$	fraction of the physical volume	1
16	16	COMP otherwise ϕ_{tough}	ϕ_{phys}	physical porosity, referring to V_{phys}	1
17	17		ϕ_{tough}	internal porosity of TOUGH, referring to V_{tough}	1
18	18	FISS	ϕ_{fiss}	porosity of a fissure	1
19	19	FISS	k_{fiss}	fissure permeability	Pa
20	20	FISS	p_{thr}	pressure Threshold	Pa
21	21	COMP	K	rate of convergence	1/s
22	22	CORRO	g	grade of canister corrosion (weighted average over sources)	1
23	23	CORRO	Q	rate of gas generation	mol/s
24	24	CORRO	m_{can}	canister water mass	kg
25	25	CORFL	g	grade of seal corrosion	1
26	26	TFC		TOUGH2-GRS/TFC: SIGMAJVEC TOUGH2-MP-GRS: outflow gas (x-component)	Pa kg/m ² /s
27	27	TFC		TOUGH2-GRS/TFC: SIGMEDVEC TOUGH2-MP-GRS: outflow gas (y-component)	Pa kg/m ² /s
28	28	TFC		TOUGH2-GRS/TFC: SIGMINVEC TOUGH2-MP-GRS: outflow gas (z-component)	Pa kg/m ² /s
29	29	TFC		TOUGH2-GRS/TFC: ACTVOLVEC TOUGH2-MP-GRS: outflow liq. (x-component)	Pa kg/m ² /s

No TOUGH2-GRS	No TOUGH2-MP-GRS	Module (0 printed if inactive)	Parameter	Description	Unit
30	30	TFC		TOUGH2-GRS/TFC: MINEFFSTRESS TOUGH2-MP-GRS: outflow liq. (y-component)	Pa kg/m ² /s
31	31	TFC		TOUGH2-GRS/TFC: MEANEFFSTRESS TOUGH2-MP-GRS: outflow liq. (z-component)	Pa kg/m ² /s
32	32	TFC		TOUGH2-GRS/TFC: PERFAC TOUGH2-MP-GRS: 0	Pa
33	33	EOS7R	X_{RN1}^{gas}	mass fraction of RN 1 in the gas phase	1
34	34	EOS7R	X_{RN1}^{liq}	mass fraction of RN 1 in the liquid phase	1
35	35	EOS7R	X_{RN2}^{gas}	mass fraction of RN 2 in the gas phase	1
36	36	EOS7R	X_{RN2}^{liq}	mass fraction of RN 2 in the liquid phase	1
37	37			number of maximal residua since last print out	1
38	38			Condition of aggregation (1: gas phase only; 2: two-phase; 3: liquid phase only)	1
39	39		$\frac{dP_{cap}}{dS_{liq}}$	dPcap/dSliq (for elements with two-phase condition only; always positive)	Pa
<i>The following lines are repeated for each radionuclide of the RN module</i>					
40+7*(i-1)	40+6*(i-1)	RN	m_{RNi}^{tot}	mass of RN i (0 for inactive elements)	kg
41+7*(i-1)	41+6*(i-1)	RN	X_{RNi}^{gas}	mobile concentration of. RN i in the gas phase	1
42+7*(i-1)	42+6*(i-1)	RN	X_{RNi}^{liq}	mobile concentration of. RN i in the liquid phase	1
43+7*(i-1)	43+6*(i-1)	RN	m_{RNi}^{gas}	mobile mass of RN i in the gas phase(0 for inactive elements)	kg
44+7*(i-1)	44+6*(i-1)	RN	m_{RNi}^{liq}	mobile mass of RN i in the liquid phase(0 for inactive elements)	kg
45+7*(i-1)	45+6*(i-1)	RN	m_{RNi}^{ads}	adsorped mass of RN I (0 for inactive elements)	kg
46+7*(i-1)		RN		OutflowAdv - OutflowDiff	kg/s

17.2 Global printouts for connections (CON_MAIN)

Global printouts are generated at user-defined times (which are specified in data blocks TIMES or PTIME) as well as on the first and last time step. The printout to file CON_MAIN contains connection-specific output using the same format as the time series files `time step number, time, [element index, [variables, ...], ...]`. If `MOPR(24)=0` (default) the diffusive flux in gas is 0 and the outputted diffusive flux in liquid holds the full multiphase diffusive flux. For `MOPR(24)=1` the diffusive flow is calculated for each phase separately. The fluxes are positive if flow is directed from the second to the first element of a connection.

Tab. 17.2 Connection-specific parameters in TOUGH2-GRS

No	Module (0 printed if inactive)	Parameter	Description	Unit
1		Q^{heat}	heat flow	J/s
2		E_s	specific energy	J/kg
3		Q^{tot}	Total mass flow	kg/s
4		Q^{gas}	mass flow in the gas phase	kg/s
5		Q^{liq}	mass flow in the liquid phase	kg/s
6		$Q_{\text{brine}}^{\text{liq}}$	Total mass flow	kg/s
7		v_{gas}	pore velocity in the gas phase	m/s
8		v_{liq}	pore velocity in the liquid phase	m/s
9	EOS7R	$Q_{\text{RN1}}^{\text{adv,gas}}$	advective flow of RN1 (gas phase)	kg/s
10	EOS7R	$Q_{\text{RN2}}^{\text{adv,gas}}$	advective flow of RN2 (gas phase)	kg/s
11	EOS7R	$Q_{\text{RN1}}^{\text{adv,liq}}$	advective flow of RN1 (liquid phase)	kg/s
12	EOS7R	$Q_{\text{RN2}}^{\text{adv,liq}}$	advective flow of RN2 (liquid phase)	kg/s
13		$Q_{\text{H}_2\text{O}}^{\text{dif,gas}}$	diffusive flow of water (gas phase)	kg/s
14		$Q_{\text{brine}}^{\text{dif,gas}}$	diffusive flow of brine (gas phase)	kg/s
15		$Q_{\text{air}}^{\text{dif,gas}}$	diffusive flow of air (gas phase)	kg/s
16	EOS7R	$Q_{\text{RN1}}^{\text{dif,gas}}$	diffusive flow of RN1 (gas phase)	kg/s
17	EOS7R	$Q_{\text{RN2}}^{\text{dif,gas}}$	diffusive flow of RN2 (gas phase)	kg/s
18		$Q_{\text{H}_2\text{O}}^{\text{dif,liq}}$	diffusive flow of water (liquid phase)	kg/s
19		$Q_{\text{brine}}^{\text{dif,liq}}$	diffusive flow of brine (liquid phase)	kg/s
20		$Q_{\text{air}}^{\text{dif,liq}}$	diffusive flow of air (liquid phase)	kg/s
21	EOS7R	$Q_{\text{RN1}}^{\text{dif,liq}}$	diffusive flow of RN1 (liquid phase)	kg/s
22	EOS7R	$Q_{\text{RN2}}^{\text{dif,liq}}$	diffusive flow of RN2 (liquid phase)	kg/s
<i>The following lines are repeated for each radionuclide of the RN module</i>				
23+5*(i-1)	RN	$Q_{\text{RN } i}^{\text{tot}}$	mass flow of RN i	kg/s
24+5*(i-1)	RN	$Q_{\text{RN } i}^{\text{adv,gas}}$	advective flow of RN i (gas phase)	kg/s
25+5*(i-1)	RN	$Q_{\text{RN } i}^{\text{dif,gas}}$	diffusive flow of RN i (gas phase)	kg/s
26+5*(i-1)	RN	$Q_{\text{RN } i}^{\text{adv,liq}}$	advective flow of RN i (liquid phase)	kg/s
27+5*(i-1)	RN	$Q_{\text{RN } i}^{\text{dif,liq}}$	diffusive flow of RN i (liquid phase)	kg/s

17.3 Time series for elements (FOFT)

These printouts are generated for user-defined elements specified in data block FOFT. The frequency of printouts can be customized by data block CNTRL.

Tab. 17.3 Element-specific parameters in FOFT

No	Module (0 printed if inactive)	Parameter	Description	Unit
1		P_{gas}	gas pressure	Pa
2		$P_{\text{liq}} = P_{\text{gas}} + P_{\text{cap}}$	liquid pressure	Pa
3		S_{gas}	gas saturation	1
4		S_{liq}	liquid saturation	1
5		X_{brine}	brine concentration	1
6		T	temperature	°C
7		$-P_{\text{cap}}$	capillary pressure (in TOUGH2 P_{cap} is negative thus the output is positive)	Pa
8		$P_{\text{pot}} = P_{\text{liq}} - z g \rho_{\text{liq}}$	pressure potential (only a potential if density is constant)	Pa
9		ρ_{gas}	density of the gas phase	kg/m ³
10		ρ_{liq}	density of the liquid phase	kg/m ³
11		μ_{gas}	viscosity of the gas phase	Pa s
12		μ_{liq}	viscosity of the liquid phase	Pa s
13		k	intrinsic permeability (for ISO=1) multiplied by the area reduction factor $V_{\text{phys}}/V_{\text{tough}}$	m ²
14		V_{tough}	initial element volume	m ³
15	COMP otherwise 1	$V_{\text{phys}}/V_{\text{tough}}$	fraction of the physical element volume $V_{\text{phys}}/V_{\text{tough}}$	1
16	COMP otherwise ϕ_{tough}	ϕ_{phys}	physical porosity, referring to V_{phys}	1
17		ϕ_{tough}	internal porosity of TOUGH, referring to V_{tough}	1
18	FISS	ϕ_{fiss}	fissure porosity	1
19	FISS	k_{fiss}	fissure permeability	m ²
20	FISS	p_{thr}	pressure threshold	Pa
21	COMP	K	rate of convergence	1/s
22	CORRO	g	grade of corrosion (weighted average over sources)	1
23	CORRO	Q	gas generation rate	mol/s
24	CORRO	m_{can}	canister water mass	kg
25	CORFL	g	grade of corrosion	1
26	EOS7R	$X_{\text{RN1}}^{\text{gas}}$	mass fraction of RN 1 in the gas phase	1
27	EOS7R	$X_{\text{RN1}}^{\text{liq}}$	mass fraction of RN 1 in the liquid phase	1
28	EOS7R	$X_{\text{RN2}}^{\text{gas}}$	mass fraction of RN 2 in the gas phase	1

No	Module (0 printed if inactive)	Parameter	Description	Unit
29	EOS7R	X_{RN2}^{liq}	mass fraction of RN 2 in the liquid phase	1
30		$m_{H_2O}^{gas}$	mass of water in the gas phase	kg
31		$m_{H_2O}^{liq}$	mass of water in the liquid phase	kg
32		m_{brine}^{gas}	mass of brine in the gas phase	kg
33		m_{brine}^{liq}	mass of brine in the liquid phase	kg
34		m_{air}^{gas}	mass of air in the gas phase	kg
35		m_{air}^{liq}	mass of air in the liquid phase	kg
36	EOS7R	m_{RN1}^{gas}	mass of RN1 in the gas phase	kg
37	EOS7R	m_{RN1}^{liq}	mass of RN1 in the liquid phase	kg
38	EOS7R	m_{RN2}^{gas}	mass of RN2 in the gas phase	kg
39	EOS7R	m_{RN2}^{liq}	mass of RN2 in the liquid phase	kg
40	EOS7R	m_{RN1}^{ads}	adsorbed mass of RN1	kg
41	EOS7R	m_{RN2}^{ads}	adsorbed mass of RN2	kg
<i>The following lines are repeated for each radionuclide of the RN module</i>				
42+6*(i-1)	RN	$m_{RN i}^{tot}$	mass of RN i (0 for inactive elements)	kg
43+6*(i-1)	RN	$X_{RN i}^{gas}$	concentration of mobile RN i in the gas phase	1
44+6*(i-1)	RN	$X_{RN i}^{liq}$	concentration of mobile RN i in the liquid phase	1
45+6*(i-1)	RN	$m_{RN i}^{gas}$	mass of mobile RN i in the gas phase (0 for inactive elements)	kg
46+6*(i-1)	RN	$m_{RN i}^{liq}$	mass of mobile RN i in the liquid phase (0 for inactive elements)	kg
47+6*(i-1)	RN	$m_{RN i}^{ads}$	adsorbed mass of RN I (0 for inactive elements)	kg

17.4 Time series for connections (COFT)

These printouts are generated for user-defined connections specified in data block COFT. The frequency of printouts can be customized by data block CNTRL. See chapter 0 for remarks on the effect of input parameter $MOP(24)$ of data block PARAM.

Tab. 17.4 Connection-specific parameters in COFT

No (KDATA \neq 4)	No (KDATA= 4)	Module (0 printed if inactive)	Parameter	Description	Unit
1	1		Q^{gas}	mass flow in the gas phase	kg/s
2	2		Q^{liq}	mass flow in the liquid phase	kg/s
3	3		Q^{heat}	heat flow	J/s
	4	EOS7R	$Q_{RN1}^{adv,gas}$	advective flow of RN1 (gas phase)	kg/s
	5	EOS7R	$Q_{RN1}^{adv,liq}$	advective flow of RN1 (liquid phase)	kg/s
	6	EOS7R	$Q_{RN1}^{adv,tot}$	advective flow of RN1 (both phases)	kg/s
	7	EOS7R	$Q_{RN2}^{adv,gas}$	advective flow of RN2 (gas phase)	kg/s
	8	EOS7R	$Q_{RN2}^{adv,liq}$	advective flow of RN2 (liquid phase)	kg/s
	9	EOS7R	$Q_{RN2}^{adv,tot}$	advective flow of RN2 (both phases)	kg/s
	10	EOS7R	$Q_{RN1}^{dif,gas}$	diffusive flow of RN1 (gas phase)	kg/s
	11	EOS7R	$Q_{RN2}^{dif,gas}$	diffusive flow of RN2 (gas phase)	kg/s
	12	EOS7R	$Q_{RN1}^{dif,liq}$	diffusive flow of RN1 (liquid phase)	kg/s
	13	EOS7R	$Q_{RN2}^{dif,liq}$	diffusive flow of RN2 (liquid phase)	kg/s
4	14	EOS7R	Q_{RN1}^{tot}	total mass flow RN1 (advection and diffusion)	kg/s
5	15	EOS7R	Q_{RN2}^{tot}	total mass flow RN2 (advection and diffusion)	kg/s
<i>The following lines are repeated for each radionuclide if the RN module is active</i>					
5+i	16+5*(i-1)	RN	$Q_{RN i}^{tot}$	total mass flow RN i	kg/s
	17+5*(i-1)	RN	$Q_{RN i}^{adv,gas}$	advective flow of RN i (gas phase)	kg/s
	18+5*(i-1)	RN	$Q_{RN i}^{adv,liq}$	advective flow of RN i (liquid phase)	kg/s
	19+5*(i-1)	RN	$Q_{RN i}^{dif,gas}$	diffusive flow of RN i (gas phase)	kg/s
	20+5*(i-1)	RN	$Q_{RN i}^{dif,liq}$	diffusive flow of RN i (liquid phase)	kg/s

17.5 Time series for sinks and sources (GOFT)

These printouts are generated for user-defined sinks and sources specified in data block GOFT.

Tab. 17.5 Sink- and source-specific parameters in GOFT.

No	Parameter	Description	Unit
1	N	generated component	1
2	\dot{m}	mass generation rate	kg/s
3	\dot{Q}	heat generation rate	J/s
4	$\int_0^t \dot{m} dt$	generated mass at time t	kg
5	$\int_0^t \dot{Q} dt$	generated heat at time t	J

17.6 Time series for domains (DOFT)

These printouts are generated for user-defined domains (rocks) in data block DOFT. The first domain of the output is the entire domain of active elements, which is not specified in the input data block DOFT. For this reason the first domain specified in data block DOFT corresponds to the second domain in the output.

Tab. 17.6 Material-specific parameters in DOFT

No. for KDATA ≠ 4	No. for KDATA = 4	Module (0 if inactive)	Parameter	Description	Unit
1	1	CORRO	N^{gas}	amount of gas produced by corrosion	mol
2	2	CORRO	m_{can}	canister water mass	kg
3	3	PRLIM	V_{esc}	gas lost due to clipping	m ³
4	4		$P_{\text{gas,max}}$	maximal gas pressure	Pa
5	5		$N_{\text{gas,max}}$	material index for the location of maximal gas pressure	
	6	EOS7R	m_{RN1}/V_i	mass of RN1 per volume of material i	kg/m ³
	7	EOS7R	m_{RN2}/V_i	mass of RN2 per volume of material i	kg/m ³
	8	EOS7R	$R_{\text{max,RN1}}$	maximal residuum of RN1	
	9	EOS7R	$R_{\text{max,RN2}}$	maximal residuum of RN2	
	10	EOS7R	$\rho_{\text{max,RN1}}$	density of RN1 for material with maximal residuum	kg/m ³
	11	EOS7R	$\rho_{\text{max,RN2}}$	density of RN2 for material with maximal residuum	kg/m ³
	12 – 15			<i>obsolete</i>	
6	16		$m_{\text{H}_2\text{O}}^{\text{gas}}$	mass of water in the gas phase	kg
7	17		$m_{\text{H}_2\text{O}}^{\text{liq}}$	mass of water in the liquid phase	kg
8	18		$m_{\text{brine}}^{\text{gas}}$	mass of brine in the gas phase	kg
9	19		$m_{\text{brine}}^{\text{liq}}$	mass of brine in the liquid phase	kg
10	20		$m_{\text{air}}^{\text{gas}}$	mass of air in the gas phase	kg
11	21		$m_{\text{air}}^{\text{liq}}$	mass of air in the liquid phase	kg
12	22	EOS7R	$m_{\text{RN1}}^{\text{gas}}$	mass of RN1 in the gas phase	kg
13	23	EOS7R	$m_{\text{RN1}}^{\text{liq}}$	mass of RN1 in the liquid phase	kg
14	24	EOS7R	$m_{\text{RN2}}^{\text{gas}}$	mass of RN2 in the gas phase	kg
15	25	EOS7R	$m_{\text{RN2}}^{\text{liq}}$	mass of RN2 in the liquid phase	kg
<i>The following lines are repeated for each radionuclides of the RN module</i>					
15+i	26+3*(i-1)	RN	$m_{\text{RN } i}^{\text{tot}}$	mass of RN i (0 for inactive elements)	kg
	27+3*(i-1)	RN	$m_{\text{RN } i}^{\text{gas}}$	mobile mass of RN i in the gas phase	kg
	28+3*(i-1)	RN	$m_{\text{RN } i}^{\text{liq}}$	mobile mass of RN i in the liquid phase	kg

References

GRS-A reports have been sponsored by the Federal Ministry for the Environment, Nature Conservation and Nuclear Safety (BMU). Quoting from these reports, reproducing them in whole or in parts or making them accessible to third parties requires the consent of BMU.

- /BFS 09/ Bundesamt für Strahlenschutz (BfS): Sicherheitsanalyse für das verfüllte und verschlossene Endlager mit dem Programmpaket EMOS. P278, BfS-KZL: 9M/23210051/EG/RB/0056/00, 27 March 2009.
- /FIS 01/ Fischer-Appelt, K., Fischer, H., Javeri, V., Martens, K.-H., Röhlig, K.-J., Eugen, S.: Implementierung von nichtlinearen Sorptionsansätzen in die Transportrechenprogramme MARNIE, NAMMU und TOUGH2 und deren Überprüfung. Gesellschaft für Anlagen- und Reaktorsicherheit (GRS) mbH, GRS-A-2897, 1 January 2001.
- /GEN 80/ Genuchten, M. T. van: A Closed-form Equation for Predicting the Hydraulic Conductivity of Unsaturated Soils. Soil Science Society of America Journal, Bd. 44, Nr. 5, pp. 892–898, DOI 10.2136/sssaj1980.03615995004400050002x, 1980.
- /GRA 14/ Grant, S. A., Bachmann, J.: Effect of Temperature on Capillary Pressure. Ed.: www.researchgate.net, available from , as at 2014.
- /HOT 17/ Hotzel, S., Navarro, M., Seher, H.: QS-Handbuch für den Programmcode TOUGH2-GRS. GRS-401, ISBN 978-3-944161-82-2, Gesellschaft für Anlagen- und Reaktorsicherheit (GRS) gGmbH: Köln, 2017.
- /JAV 95/ Javeri, V.: Orientierende Analysen zum Nuklidtransport durch Naturkonvektion; Gesteinskonvergenz und Dispersion in porösen Medien mit dem Rechenprogramm TOUGH2. Gesellschaft für Anlagen- und Reaktorsicherheit (GRS) mbH, GRS-A-2240: Köln, 1995.

- /JAV 01/ Javeri, V.: Dreidimensionale Analysen zum Nuklidtransport bei salzanteilabhängiger Adsorption in einem porösen Medium mit dem Rechenprogramm TOUGH2. Gesellschaft für Anlagen- und Reaktorsicherheit (GRS) mbH, GRS-A-2864: Köln, 2001.
- /JAV 02/ Javeri, V.: Analysen zum Nuklidtransport bei variabler Salinität und nichtlinearer Adsorption in der stark heterogenen Geosphäre der Gorlebener Rinne. Gesellschaft für Anlagen- und Reaktorsicherheit (GRS) mbH, GRS-A-3038: Köln, 2002.
- /JUN 17/ Jung, Y., Pau, G. S. H., Finsterle, S., Pollyea, R. M.: TOUGH3, A new efficient version of the TOUGH suite of multiphase flow and transport simulators. Computers and Geosciences, Bd. 108, pp. 2–7, DOI 10.1016/j.cageo.2016.09.009, 2017.
- /KOC 12/ Kock, I., Eickemeier, R., Frieling, G., Heusermann, S., Knauth, M., Minkley, W., Navarro, M., Nipp, H.-K., Vogel, P.: Integritätsanalyse der geologischen Barriere, Bericht zum Arbeitspaket 9.1, Vorläufige Sicherheitsanalyse für den Standort Gorleben. Gesellschaft für Anlagen- und Reaktorsicherheit (GRS) mbH, GRS-286, 301 p., ISBN 978-3-939355-62-5: Köln, 2012.
- /KOC 16/ Kock, I., Frieling, G., Navarro, M.: Fluidströmung und Radionuklidtransport in komplexen Endlagerbergwerken, Synthesebericht Teil 1/2, Zweiphasenfluss in einem salinaren Endlager am Beispiel des ERAM. GRS-399, ISBN 978-3-944161-80-8, Gesellschaft für Anlagen- und Reaktorsicherheit (GRS) gmbH: Köln, 2016.
- /KRÖ 09/ Kröhn, K. P., Stührenberg, D., Herklotz, M., Heemann, U., Lerch, C., Xie, M.: Restporosität und -permeabilität von kompaktierendem Salzgrusversatz in einem HAW-Endlager - Phase 1. Gesellschaft für Anlagen- und Reaktorsicherheit (GRS) mbH, GRS-254, 266 p., ISBN 978-3-939355-29-8, 2009.

- /LAR 13/ Larue, P.-J., Baltés, B., Fischer, H., Frieling, G., Kock, I., Navarro, M., Seher, H.: Radiologische Konsequenzenanalyse, Bericht zum Arbeitspaket 10, Vorläufige Sicherheitsanalyse für den Standort Gorleben. GRS-289, 267 p., ISBN 978-3-939355-65-6, Gesellschaft für Anlagen- und Reaktorsicherheit (GRS) mbH: Köln, 2013.
- /LBNL 16/ Lawrence Berkeley National Laboratory (LBNL): TOUGH2 V2.0: Bugs and Fixes. Available from <http://esd1.lbl.gov/research/projects/tough/software/BugFixes.html>, retrieved on 9 February 2016.
- /LEV 41/ Leverett, M. C.: Capillary behaviour in porous solids. Transactions of the AIME, Bd. 142, pp. 159–172, 1941.
- /NAV 08/ Navarro, M., Baltés, B., Beuth, T., Bracke, G., Fischer, H., Fischer-Appelt, K., Hotzel, S., Javeri, V., Kindt, A., Lambers, L., Larue, P.-J., McStocker, B., Oppermann, U., Schrödl, E.: Verfolgung und Bewertung der Fortentwicklung des Standes von Wissenschaft und Technik beim Nachweis der Langzeitsicherheit von Endlagern, Abschlussbericht zum Vorhaben SR 2548. Gesellschaft für Anlagen- und Reaktorsicherheit (GRS) mbH, GRS-A-3418: Köln, 2008.
- /NAV 09/ Navarro, M.: Simulating the migration of repository gases through argillaceous rock by implementing the mechanism of pathway dilation into the code TOUGH2 (TOUGH2-PD), PAMINA project, public milestone 3.2.14. Gesellschaft für Anlagen- und Reaktorsicherheit (GRS) mbH, Community Research, 59 p., European Commission (EC): Brüssel, September 2009.
- /NAV 13a/ Navarro, M.: Modelling Gas and Water Flow Through Dilating Pathways in Opalinus Clay, The HG-C and HG-D Experiments, A study within the Euratom 7th Framework Programme Project FORGE. Gesellschaft für Anlagen- und Reaktorsicherheit (GRS) mbH, GRS-306, ISBN 978-3-939355-85-4: Cologne, 2013.
- /NAV 13b/ Navarro, M.: Handbuch zum Code TOUGH2-GRS.00a, Erweiterungen des Codes TOUGH2 zur Simulation von Strömungs- und Transportprozessen in Endlagern. Gesellschaft für Anlagen- und Reaktorsicherheit (GRS) mbH, GRS-310, 75 p., ISBN 978-3-939355-89-2: Köln, 2013.

- /NAV 13c/ Navarro, M.: Die vereinfachte Berechnung der Konvergenzrate salzgrusverfüllter Hohlräume im Steinsalz. GRS-307, 47 p., ISBN 978-3-939355-86-1, Gesellschaft für Anlagen- und Reaktorsicherheit (GRS) mbH: Köln, 2013.
- /NAV 15/ Navarro, M.: Speeding up the iterative solvers of the T2SOLV solver package, A presentation at the TOUGH-Symposium 2015 at the Lawrence Berkeley National Laboratories. As at 2015, available from http://tough.lbl.gov/assets/docs/support/Speeding_up_LINEQ.pdf, retrieved on 04.05.16.
- /NAV 16a/ Navarro, M., Eckel, J.: TOUGH2-GRS, Version 1, User Manual. GRS-403, 87 p., ISBN 978-3-944161-84-6, Gesellschaft für Anlagen- und Reaktorsicherheit (GRS) gGmbH: Köln, July 2016.
- /NAV 16b/ Navarro, M., Fischer, H., Seher, H., Weyand, T. (Eds.): Ansätze zur Simulation der Zweiphasenströmung in salinaren Endlagern mit dem Code TOUGH2-GRS, Bericht im Vorhaben ZIESEL, Zweiphasenfluss in einem salinaren Endlager am Beispiel des ERAM. GRS-398, 139 p., ISBN 978-3-944161-79-2, Gesellschaft für Anlagen- und Reaktorsicherheit (GRS) gGmbH: Köln, October 2016.
- /NAV 18a/ Navarro, M., Eckel, J., Fischer, H., Hotzel, S., Kock, I.: Test Handbook, TOUGH2-GRS Version 2, TOUGH2-MP-GRS Version 0. GRS-402, ISBN 978-3-944161-83-9, Gesellschaft für Anlagen- und Reaktorsicherheit (GRS) gGmbH: Köln, 2018.
- /NAV 18b/ Navarro, M.: User Manual, TOUGH2-GRS Version 2, TOUGH2-MP-GRS Version 0. Gesellschaft für Anlagen- und Reaktorsicherheit (GRS) gGmbH, 2018.
- /NOS 05/ Noseck, U., Brewitz, W., Becker, D.-A., Buhmann, D., Fahrenholz, C., Fein, E., Hirsekorn, R.-P., Keesmann, S., Kröhn, K.-P., Müller-Lyda, I., Rübel, A., Schneider, A., Storck, R.: Wissenschaftliche Grundlagen zum Nachweis der Langzeitsicherheit von Endlagern. Gesellschaft für Anlagen- und Reaktorsicherheit (GRS) mbH, GRS-204, 205 p., ISBN 3-931995-71-2: Köln, Garching b. München, Berlin, Braunschweig, 2005.

- /PRU 99/ Pruess, K., Oldenburg, C., Moridis, G.: TOUGH2 User's Guide, Version 2.0. Lawrence Berkeley National Laboratory (LBNL), LBNL-43134, 198 p.: Berkeley, California, USA, 1 November 1999, revised September 2012.
- /SEH 16/ Seher, H., Navarro, M.: SITA, Version 0, A simulation and code testing assistant for TOUGH2 and MARNIE. GRS-400, 78 p., ISBN 978-3-944161-81-5, Gesellschaft für Anlagen- und Reaktorsicherheit (GRS) gGmbH: Köln, June 2016.
- /STE 85/ Stelte, N.: Analytische Approximation der Konvergenzrate salzgrusversetzter und unter hydraulischem Druck stehender Hohlräume im Salzgestein. In: Projekt Sicherheitsstudien Entsorgung (PSE) (Ed.): Einzeluntersuchungen zur Radionuklidfreisetzung aus einem Modellsalzstock, Fachband 15. pp. 108–141, TU Berlin: Berlin, 1985.
- /STO 80/ Stoer, J., Bulirsch, R.: Introduction to Numerical Analysis. 609 p., ISBN 978-1-4757-5594-7, Springer New York: New York, NY, 1980.
- /ZHA 08/ Zhang, K., Wu, Y.-S., Pruess, K.: User's Guide for TOUGH2-MP - A Massively Parallel Version of the TOUGH2 Code. Lawrence Berkeley National Laboratory (LBNL), LBNL-315E: Berkeley, California, USA, 1 May 2008.

List of Figures

Fig. 3.1	Models for drift sections with (A) and without (B) vertical discretisation.....	18
Fig. 14.1	Relationship between saturation limits of the RANGE and CORRO modules.....	67

List of Tables

Tab. 2.1	Fortran modules of TOUGH2-GRS and TOUGH2-MP-GRS	10
Tab. 2.2	Restart files and their content	14
Tab. 4.1	Input format of data block CNTRL.....	24
Tab. 5.1	Input format of data block COMP	29
Tab. 6.1	Input format of data block CORFL	35
Tab. 7.1	Input format of data block CORRO	45
Tab. 8.1	Input format of data block DEGRA.....	47
Tab. 9.1	Input format of data block DOFT	49
Tab. 10.1	Input format of data block FISS.....	55
Tab. 11.1	Input format of data block GCOMP	60
Tab. 12.1	Input format of data block PRLIM.....	62
Tab. 13.1	Input format of data block PTIME.....	63
Tab. 14.1	Input format of data block RANGE.....	68
Tab. 15.1	Input format of data block RELA	71
Tab. 16.1	Input format of data block RN	84
Tab. 16.2	Commands of module RN.....	85
Tab. 17.1	Element-specific output parameters of TOUGH2-GRS	88
Tab. 17.2	Connection-specific parameters in TOUGH2-GRS	91
Tab. 17.3	Element-specific parameters in <code>FOFT</code>	92

Tab. 17.4	Connection-specific parameters in COFT	94
Tab. 17.5	Sink- and source-specific parameters in GOFT	95
Tab. 17.6	Material-specific parameters in DOFT.....	96

Acknowledgements

The author wants to thank Jens Eckel for implementing the Bulirsch-Stoer solver for the RN module. Many thanks to Stephan Hotzel who has formulated the new mobilization models of the RN module.

**Gesellschaft für Anlagen-
und Reaktorsicherheit
(GRS) gGmbH**

Schwertnergasse 1
50667 Köln

Telefon +49 221 2068-0

Telefax +49 221 2068-888

Boltzmannstraße 14

85748 Garching b. München

Telefon +49 89 32004-0

Telefax +49 89 32004-300

Kurfürstendamm 200

10719 Berlin

Telefon +49 30 88589-0

Telefax +49 30 88589-111

Theodor-Heuss-Straße 4

38122 Braunschweig

Telefon +49 531 8012-0

Telefax +49 531 8012-200

www.grs.de